Science
AAAS

Supplementary Materials for

Bioadhesive polymer semiconductors and transistors for intimate biointerfaces

Nan Li[1,2], Yang Li[1], Zhe Cheng[2], Youdi Liu[1], Yahao Dai[1], Seounghun Kang[1], Songsong Li[1], Naisong Shan[1], Shinya Wai[1], Aidan Ziaja[1], Yunfei Wang[3], Joseph Strzalka[4], Wei Liu[1], Cheng Zhang[1], Xiaodan Gu[3], Jeffrey A. Hubbell[1,5,6], Bozhi Tian[2], Sihong Wang[1,7]*

Corresponding author: sihongwang@uchicago.edu

The PDF file includes:

Other Supplementary Materials for this manuscript include the following:

Materials and Methods

Materials

The chemicals used in the study, including tetra(ethylene glycol), acryloyl chloride, triethylamine, succinic anhydride, 4-dimethylaminopyridine (DMAP), *N*-hydroxysuccinimide (NHS), 2,5-bis(trimethylstannyl)thiophene, trimethyl(phenyl)tin, bromobenzene, 2-hydroxy-2-methyl-propiophenone, anhydrous dichloromethane (DCM), anhydrous chloroform, and anhydrous chlorobenzene were purchased from Sigma-Aldrich and used without further purification. Tetraethylene glycol dimethylacrylate was purchased from Polysciences Inc. 1-ethyl-3-(3-dimethylaminopropyl)carbodiimide hydrochloride (EDC) was purchased from Oakwood Chemical. 5,5'-Dibromo-3,3'-bis(2-(2-(2-methoxyethoxy)ethoxy)ethoxy)-2,2'-bithiophene was purchased from SunaTech Inc. SEBS was obtained from Asahi Kasei. The thermoplastic polyurethane (TPU) was obtained from BASF.

Characterizations

Microwave polymerization was conducted using a Biotage Initiator +. Nuclei magnetic resonance (NMR) spectra were recorded on a Bruker Avance III HD console spectrometer (^{1}H 400 MHz, ^{13}C 100 MHz) at 293 K. Chemical shifts are given in parts per million (ppm) with respect to tetramethylsilane as an internal standard, and coupling constants (*J*) are given in Hertz (Hz). High-resolution mass spectra (HR-MS) were recorded on an Agilent 6530 LC Q-TOF mass spectrometer using electrospray ionization with fragmentation voltage set at 70 V and processed with an Agilent MassHunter Operating System. Number average molecular weight (M_n), weight average molecular weight (M_w), and polydispersity index (PDI) were evaluated by Tosoh EcoSEC size exclusion chromatography system (GPC) using DMF + 0.01 M LiBr as eluent (50 ºC) calibrated with polystyrene standards. The UV-Vis absorption spectra were recorded on the Shimadzu UV-3600 Plus UV-VIS-NIR spectrophotometer. The water contact angle measurement was done with a KRÜSS DSA100 drop shape analyzer. Differential scanning calorimetry (DSC) experiments were performed with a TA Instruments Discovery 2500 differential scanning calorimeter. The atomic force microscope (AFM) imaging was done with the Bruker Multimode 8 AFM. The scanning electron microscope (SEM) imaging was done with the FEI Quanta 650 FEG SEM. The depth-profiling X-ray photoelectron spectroscopy (XPS) was done with Kratos AXIS Nova with a monochromatic Al Kα X-ray source and a delay line detector (DLD) system with Ar1000+ with 10 keV to etch. Grazing-incidence X-ray diffraction (GIXD) was performed at the Advanced Photon Source at Argonne National Laboratory on beamline 8-ID-E.

Semiconducting film fabrication

The glass substrates were treated with a *n*-octadecyltrimethoxysilane (OTS) layer on the surface (*46*). P(g2T-T) polymer was dissolved in chloroform with a concentration of 5 mg/mL. For non-adhesive semiconducting polymer films, the polymer solution was directly spin-coated on the OTS-treated glass substrate at a spin speed of 1,000 r.p.m. for 1 min in a nitrogen-filled glovebox. The polymer film was finally annealed at 110 ºC for 5 min. For preparing the bioadhesive semiconductor precursor solution, a certain amount of well-dissolved p(g2T-T) polymer solution in 5 mg/mL was mixed with desired amounts of ACTEGCOOH or ACTEGNHS monomers, 0.5 wt% of 2-hydroxy-2-methyl-propiophenone (as the photoinitiator) and 0.5 wt% of tetraethylene glycol dimethylacrylate (as the crosslinker) in chloroform (Table S2). For preparing BASC polymer, the weight ratio of p(g2T-T) to ACTEGCOOH to ACTEGNHS is 1-20-20. The mixture was allowed to stir for 20 min at 60 ºC before spin-coating. The polymer solution was spin-coated

on the OTS-treated glass substrates at a spin speed of 1,000 r.p.m. for 1 min in a nitrogen-filled glovebox. The film was then photo-polymerized under 365 nm UV light for 5 min, followed by annealing at 110 °C for 5 min in a nitrogen-filled glovebox. For adhesion and mechanical characterizations of the semiconducting films, stretchable substrates were fabricated by dissolving TPU in THF with a concentration of 60 mg/mL and then drop-casting the solution on a clean glass substrate to obtain a uniform TPU film (thickness around 70 μm) after the complete evaporation of the solvent in room temperature. The semiconducting polymer precursor solution was spin-coated on the TPU substrates at a spin speed of 1,000 r.p.m. for 1 min in a nitrogen-filled glovebox. The polymer film then was photocured under 365 nm UV light for 5 min, followed by annealing at 110 °C for 5 min in the glovebox. The TPU film can be peeled off from the glass substrate.

OECT fabrication for the characterization of electrical performance

First, a glass substrate was cleaned with acetone, isopropyl alcohol, and water, successively. After that, the source/drain gold electrodes (60-nm thick) are patterned via e-beam evaporation with a metal shadow mask. The channel length (L) and width (W) are 200 μm and 4 mm, respectively. The semiconducting polymer films were transferred onto the channel area using a PDMS stamp. The electrolyte of 0.1 M NaCl solution was dropped on top of the channel. The gate electrode was served by Ag/AgCl. The performance of the fabricated OECTs were measured using Keithley 4200 under an ambient environment. The transconductances (g_{m}) were calculated from the transfer curves, as

$$g_{\mathrm{m}} = \frac{\partial I_d}{\partial V_g}$$

Electrochemical characterization

The electrochemical measurements were done using the PalmSens electrochemical workstation. The polymer solution was spin-coated on gold electrode as the working electrode. The exposed gold area was encapsulated with the epoxy resin. The EIS measurements were performed in either 0.1 M NaCl solution or 1X PBS solution, with Ag/AgCl as the reference electrode and Pt as the counter electrode. The EIS spectrum was obtained over a range of 10 kHz to 0.1 Hz with an AC 10 mV sine wave and a DC offset of 0.2 V. The analysis of the EIS data was carried out using Multitrace 4.5 software. And the volumetric capacitance was averaged from 3 samples. The mobility was calculated based on the equation $g_{\mathrm{m}} = \frac{Wd}{L}\mu C^{*}(V_{\mathrm{th}} - V_{\mathrm{g}})$, where d is the film thickness, μ is the charge-carrier mobility, C^{*} is the capacitance of the channel per unit volume, and V_{th} is the threshold voltage.

Mechanical characterization

For rheology measurement, the adhesive semiconductor precursor solution was drop-casted on a clean glass substrate and was fully polymerized under 365 nm UV light in a nitrogen-filled glovebox. The samples were then annealed at 110 °C for 10 min to fully remove the residue solvent. The final film was cut into a circular shape with a diameter of 10 mm and a thickness around 0.8 mm. The rheology test was done with TA Instruments ARES-G2 shear rheometer at room temperature.

For adhesion tests, the semiconducting polymer films were prepared on TPU substrates according to the process described above. The TPU substrates were then cut into a rectangular shape with a

length/width of 80 mm/6 mm. The semiconducting polymer occupies one end with an average length/width of 10 mm/6 mm.

The surfaces of synthetic materials including PDMS, TPU, glass, and gold were treated with primary amine groups according to procedures reported in literature (*47*).

The bio-tissues were purchased from local markets. Generally, the bio-tissues were cut into rectangular pieces and rinsed with 0.1X PBS solution and pre-dried gently with Kimwipe to remove excess water on the surface. The bio-tissues were fixed to a glass substrate at one end with Kapton tape. The bioadhesive polymers on TPU substrates were adhered to the bio-tissue surface by gently pressing of ~ 5 kPa for 1 min. All the samples were stored in a sealed bag at 4-8 ^{o}C for 2 h before the mechanical test.

The interfacial toughness was tested by the 180° peel test with a Zwick-Roell zwickiLine Z0.5 materials testing instrument. All tests were conducted with a constant peeling speed of 0.5 %/s. Interfacial toughness was calculated from the plateau force and the width of the adhered area following the corresponding ASTM standard. The shear strength was tested by the lap-shear test with a Zwick-Roell zwickiLine Z0.5 materials testing instrument. All tests were conducted with a constant tensile speed of 0.5 %/s. Shear strength was calculated by dividing the maximum force by the adhered area following the corresponding ASTM standard. The tensile strength was tested by the tensile test with a Zwick-Roell zwickiLine Z0.5 materials testing instrument. All tests were conducted with a constant tensile speed of 0.5 %/s. Tensile strength was calculated by dividing the maximum force by the adhered area following the corresponding ASTM standard.

Film-on-water (FOW) test

To prepare the thin film samples, polystyrene sulfonate (PSS, 3 wt%) aqueous solution was first spin-coated on the silicon wafer as a sacrificial layer and then the semiconductor polymer solution was spin-coated on top. The films were patterned into the dogbone or rectangular shape using ultrafast laser patterning and then released from water. Details of the tensile stage setup can be found in the previous publication (*48*). Briefly, the film was unidirectionally deformed at a strain rate of 0.04 mm/s until film fracture. Elastic modulus was obtained from the slope of the linear fit based on the elastic region from the stress-strain curve using the first 1 % strain. For the fracture toughness measurement, notched and unnotched polymer films were prepared and tested with the pure shear method. Both materials were laser-etched into an I shape with a 2 mm * 16 mm rectangular gauge, and two 2 mm * 20 mm rectangular pads. For a notched sample, an 8 mm-long notch was introduced to its center along the width direction. A strain rate of 0.02 s^{-1} was performed for the tensile test of all samples. The critical displacement for stable crack propagation was identified from the force-displacement curve of notched samples.

In vitro biocompatibility

RAW 264.7 cells, a mouse macrophage cell line, was obtained from ATCC (Cat# TIB-71) and were cultured according to instructions. RAW 264.7 cell line was routinely checked for mycoplasma contamination. For sample preparation, the BASC films were supported on SEBS substrates. p(g2T-T) film is prepared in the same way and is tested as a control sample. RAW 264.7 cells were cultured into a 48-well plate (50,000 cells per well) that was pre-coated with the films (n = 5) and incubated in a cell incubator for 24 h. The cells were carefully washed using PBS

and conducted MTT assay for measuring the cell viability. For the live/dead staining, the cells pre-incubated with the films were carefully washed using PBS and stained using LIVE/DEAD assay (Thermofisher) in a cell incubator for 15 min. The fluorescence images were taken using EVOSTM M7000 imaging system (Invitrogen).

In vivo biocompatibility

Male C57BL/6 (age 8 weeks) were purchased from Charles River Laboratory. All the animal experiments performed in this research were approved by the Institutional Animal Care and Use Committee of the University of Chicago.

The elastomer SEBS-1221 substrate with a thickness of 1 mm were prepared by drop-casting the SEBS solution in toluene onto a clean glass substrate. The adhesive polymer samples were prepared by spin-coating adhesive precursor solution in chloroform on oxygen plasma treated SEBS substrates at a spin speed of 1,000 r.p.m. for 1 min in a nitrogen-filled glovebox. The polymer films were then photocured under 365 nm UV light for 5 min, followed by annealing at 110 ^{o}C for 5 min in a nitrogen-filled glovebox. The other side of SEBS substrate was coated with the adhesive polymer in the same way. The adhesive polymer-coated SEBS substrates were then punched into circular disks with a diameter of 6 mm with biopsy. Before implantation, all the disks were sterilized with 70 % ethanol solution and UV light for 20 min each. Anaesthesia was maintained using a nose cone. The back hair was removed. The subcutaneous space was accessed by a 1-2 cm skin incision per implant in the center of the animal's back. To create space for implant placement, blunt dissection was performed from the incision towards the animal's shoulder blades. The sample was placed in the subcutaneous pocket created above the incision (n = 5). The incision was closed with interrupted sutures. After one month post the implantation, the animals were killed by CO_2 inhalation. The implanted samples were excised and collected for biocompatibility analysis.

Histological analysis (trichrome staining)

The mice skin samples were harvested at scheduled end point and incubated in 2 % PFA for 2 days at 4 ℃. The fixed skin samples were conducted paraffin embedding process and sectioned at 5 μm thickness. Trichrome staining was conducted by Human Tissue Resource Center, the University of Chicago. The slides were imaged by EVOS FL Auto (Life Technologies).

Immunofluorescence analysis

The paraffin embedded skin samples were sectioned at 5 μm, and the slides were performed with deparaffination process. The slides were incubated in perm/blocking buffer (0.3 % Triton X-100, 1 % BSA in PBS) for 3 h at room temperature. The slides were washed using 1X PBS 3 times and incubated in primary antibody solution (0.1 % tween 20 in PBS) for overnight at 4 ℃. The primary antibodies information: Anti-alpha smooth muscle Actin antibody (EPR5368, abcam) and CD68 Monoclonal Antibody (FA-11, Invitrogen). The slides were washed using 1X PBS 3 times and incubated in secondary antibody solution (0.1 % tween 20 in PBS) for 3 h at room temperature. Secondary antibody information: Donkey anti-Rat IgG (H+L) Alexa Fluro^{TM} 594 Secondary Antibody and Goat anti-Rabbit IgG Alexa Fluor^{TM} 647 Secondary Antibody (Invitrogen). Then, the slides were washed using 1X PBS 3 times and stained using DAPI. The stained skin slides were covered with mounting solution and dried for overnight in dark place. The slides were imaged by Olympus confocal microscopy system.

Fabrication of fully-bioadhesive OECT sensors

BAP adhesive precursors in chloroform were spin-coated on the tip area of oxygen plasma treated TPU substrates followed by curing at 365-nm light for 5 min and annealing at 110 ^{o}C for 5 min in a nitrogen-filled glovebox. The prepared substrates were stretched biaxially (stretched along one major direction at 80 % strain, and along the other direction for around 30 % strain) and fixed to a glass substrate. Then a PET shadow mask was attached to each substrate with openings for gate, source and drain electrodes sitting on the adhesive area. SEBS 1052 solution in toluene with a concentration of 10 mg/mL was spin-coated on the open channel as the bottom encapsulation layer. After that, the titanium/gold electrodes were fabricated through e-beam evaporation to achieve a thickness of 5 nm/80 nm. Then the mask was carefully removed. The fixed substrate was slowly released to its original shape so microcracked gold electrodes were obtained. Then, BASC films were transferred to the channel area and the gate area to serve as both the channel and gate materials. The device was flipped and the BAP adhesive precursors in chloroform were spin-coated on backside of the tip area on the TPU substrate followed by curing at 365-nm light for 5 min and annealing at 110 ^{o}C for 5 min in a nitrogen-filled glovebox. Thin SEBS 1052 films (~570 nm) were transferred with a PDMS stamp to encapsulate the exposed gold electrodes. Finally, the completed device was released from the glass substrate.

Fabrication of the non-bioadhesive OECT sensor

A TPU substrate was stretched biaxially (stretched along one major direction at 80 % strain, and along the other direction for around 30 % strain) and fixed to a glass substrate. A PET shadow mask was attached to the substrate. Then SEBS 1052 solution in toluene with a concentration of 10 mg/mL was spin-coated on the open channel as the bottom encapsulation layer. After that, titanium/gold electrodes were fabricated through e-beam evaporator with a thickness of 5 nm/80 nm. Then the mask was carefully removed. The fixed substrate was slowly released to its original shape so microcracked gold electrodes are obtained. Neat semiconducting polymer p(g2T-T) films were transferred to the channel area and the gate area to serve as both the channel and gate materials. Thin SEBS 1052 films (~570 nm) were transferred with a PDMS stamp to encapsulate the exposed gold electrodes. The device was finally released from the glass substrate.

Fabrication of the passive electrode sensor

A TPU substrate was stretched biaxially (stretched along one major direction at 80 % strain, and along the other direction for around 30 % strain) and fixed to a glass substrate. A PET shadow mask was attached to the substrate. Then SEBS 1052 solution in toluene with a concentration of 10 mg/mL was spin-coated on the open channel as the bottom encapsulation layer. After that, titanium/gold electrodes were fabricated through e-beam evaporator with a thickness of 5 nm/80 nm. Then the mask was carefully removed. The fixed substrate was slowly released to its original shape so microcracked gold electrodes are obtained. PEDOT:PSS (PH1000) blending with 1/1 weight ratio of hydrophilic polyurethane (HydroMed D4) was spin-coated on top of the electrode to lower the interfacial impedance with bio-tissues (*49, 50*). Silicon rubber adhesive was blade-coated to encapsulate the exposed gold electrodes. The device was finally released from the glass substrate.

Ex vivo ECG measurement

Isolated rat hearts were prepared following the method described previously (*51*). An adult rat (males, 300-400 g body weight, purchased from Charles River Laboratory) was heparinized and anaesthetized using open-drop exposure of isoflurane in a bell jar configuration. The heart was removed and placed in ice cold HBSS buffer, and the aorta was cannulated in preparation for use in a Langendorff set-up. Oxygenated HEPES-buffered Tyrode's solution was perfused through the cannulated aorta after passing through a heating coil and bubble trap (Radnoti). The heart was placed in a water-jacketed beaker (Fisher Scientific) to maintain a temperature of 37 °C. The perfusion pressure was maintained at 80-100 mmHg. The sinoatrial node along with the atria were removed to lower the atrioventricular node pace. The perfusion and left ventricular pressure were monitored using a BP-100 probe (iWorx) connected to the perfusion line and a water-filled balloon (Radnoti) inserted into the LV, respectively. For ECG recordings, a fully-bioadhesive (or non-bioadhesive) OECT sensor was positioned on the ventricular wall and the source-drain voltage was powered by a Keithley 2450 SourceMeter. Gentle pressure was applied on the back of the OECT device for 20 s to make sure adhesion formation. The output signals were connected to a C-ISO-256 preamplifier (iWorx). All signals (perfusion, left ventricular pressure and ECG) were amplified using an IA-400D amplifier (iWorx) and interfaced with a computer using a Digitate 1550 digitizer with Clampex software (Molecular Devices).

In vivo EMG measurement

The sciatic nerve surgery followed methods described previously (*51*). In short, an adult rat (10-24 weeks, males, purchased from Charles River Laboratory) was deeply anaesthetized with isoflurane (3-4 %). The fur was removed from the hindquarters using surgical clippers and hair removal cream. An incision across the midline was made in the skin, and the fascial plane was opened between the gluteus maximus and the anterior head of the biceps femoris, exposing the sciatic nerve. The nerve was extruded using sutures and was stimulated by bipolar silver wire electrodes (0.003 µm, A-M Systems). Biphasic electrical impulses (durations of cathodic phase, anodic phase and inter-phase interval: 0.2 ms) were generated by a potentiostat (SP-200, BioLogic) controlled with EC-Lab software. After cutting the skin open, the bioadhesive transistor was attached to the gastrocnemius medialis (GM) muscle with gentle pressure applied for 20 s. For EMG recordings, the output was connected to a C-ISO-256 preamplifier (iWorx). The EMG signal was amplified using an IA-400D amplifier (iWorx) and interfaced with a computer using a Digidata 1550 digitizer with Clampex software (Molecular Devices).

Materials synthesis

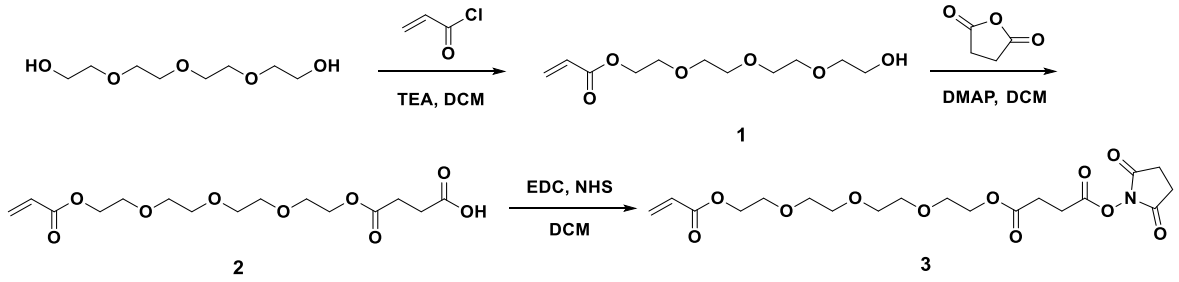

2-(2-(2-(2-hydroxyethoxy)ethoxy)ethoxy)ethyl acrylate (1)

To a round bottom flask (RBF) with a stirring bar, tetra(ethylene glycol) (103 mmol, 20 g) and triethylamine (41.2 mmol, 4.2 g) were added to 30 mL anhydrous DCM under nitrogen atmosphere

with an ice bath. Acryloyl chloride (20.6 mmol, 1.86 g) was added dropwise under stirring. Then the mixture was stirred at room temperature (r.t.) overnight. After that, the solid was filtered and the solution was washed with water. The product was extracted with DCM. The solvent was removed using rotary evaporation and purified by column chromatography (silica gel, EA/MeOH=95:5, v:v). The final product was isolated as a colorless oil (4.8 g, 94 %). ^{1}H NMR (400 MHz, $CDCl_3$) δ 6.40 (dd, *J* = 17.3, 1.4 Hz, 1H), 6.13 (dd, *J* = 17.3, 10.4 Hz, 1H), 5.81 (dd, *J* = 10.4, 1.4 Hz, 1H), 4.30 (dd, *J* = 5.5, 4.2 Hz, 2H), 3.76 – 3.67 (m, 4H), 3.67 – 3.61 (m, 8H), 3.58 (dd, *J* = 5.3, 3.8 Hz, 2H), 2.66 (s, 1H); ^{13}C NMR (101 MHz, $CDCl_3$) δ 166.16, 131.03, 128.26, 72.52, 70.66, 70.59, 70.55, 70.35, 69.13, 63.65, 61.73. HRMS (ESI) Calcd for C11H21O6 [M+H]+ : 249.1333, found 249.1334.

^{1}H NMR spectrum (400 MHz, $CDCl_3$) of compound 1

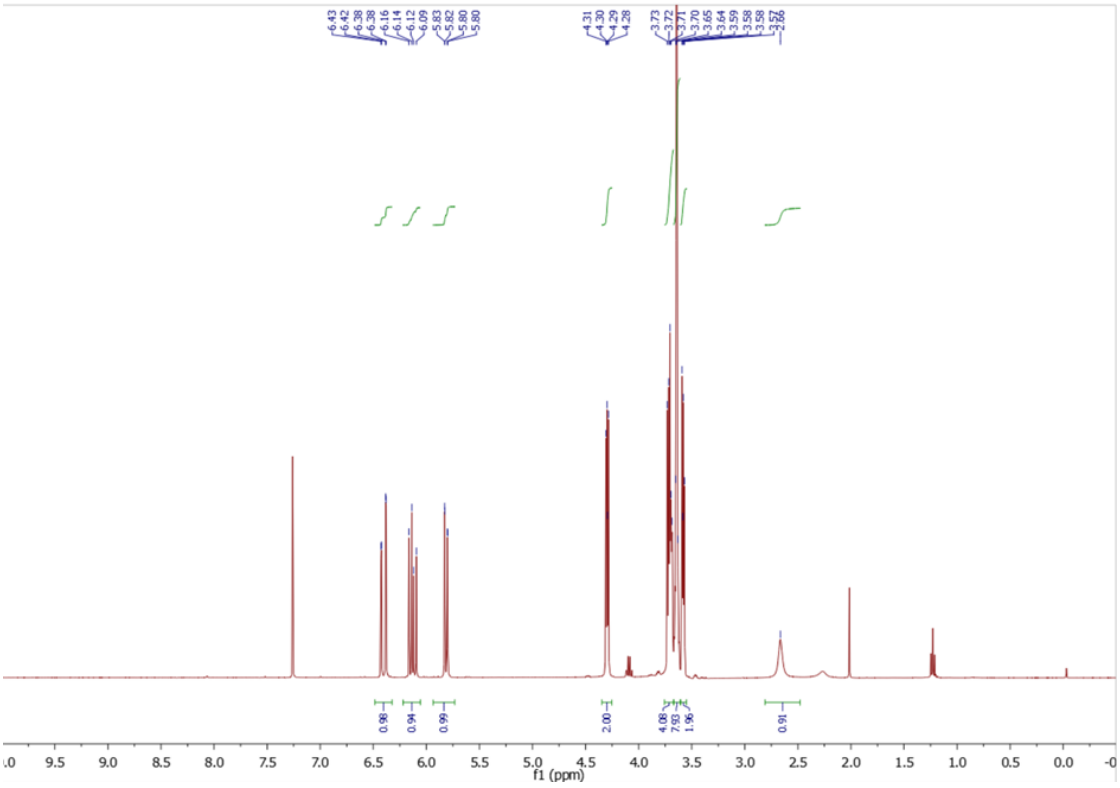

^{13}C NMR spectrum (101 MHz, $CDCl_3$) of compound 1

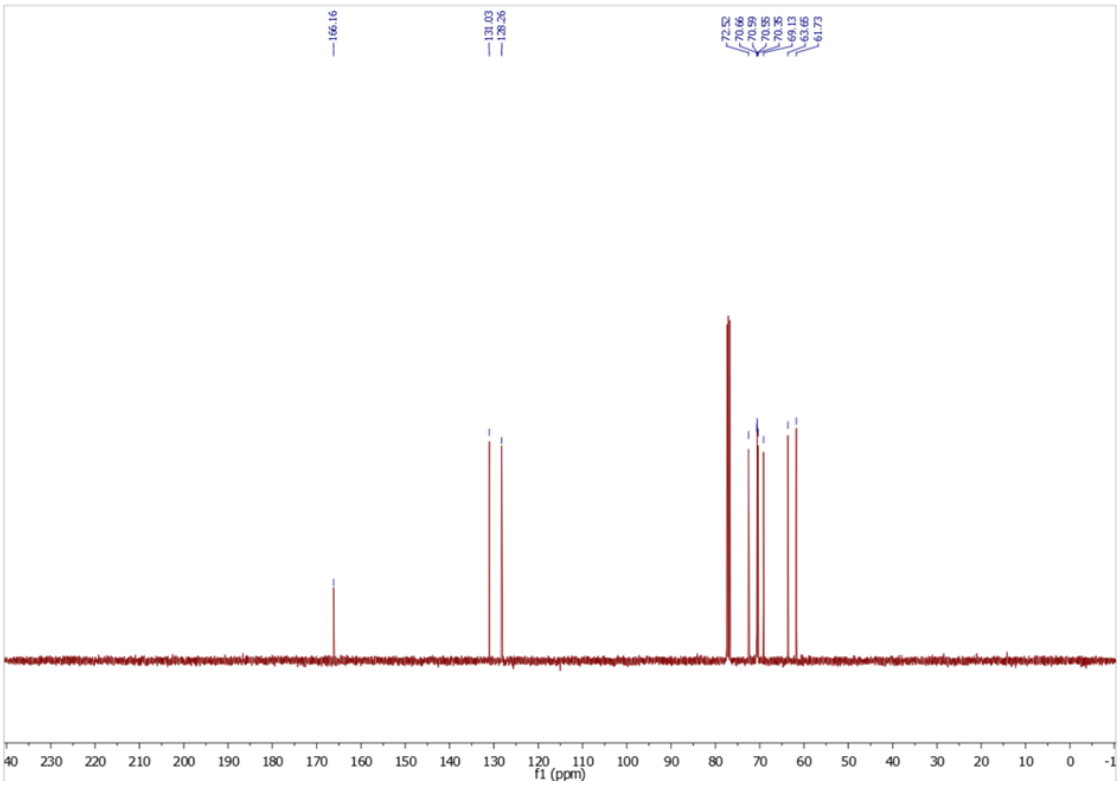

3,17-dioxo-4,7,10,13,16-pentaoxaicos-1-en-20-oic acid (2)

To a RBF with a stirring bar, **1** (16 mmol, 4 g), succinic anhydride (32 mmol, 3.2 g), and DMAP (1.1 mmol, 138 mg) were added to 40 mL anhydrous DCM under nitrogen atmosphere. The mixture was stirred at r.t. overnight. After that, the solution was washed with 1M HCl and brine successively. The product was extracted with DCM. The solvent was removed using rotary evaporation and purified by column chromatography (silica gel, EA/MeOH=95:5, v:v). The final product was isolated as a colorless oil (3.9 g, 70 %). ^{1}H NMR (400 MHz, $CDCl_3$) δ 6.43 (dd, *J* = 17.3, 1.4 Hz, 1H), 6.15 (dd, *J* = 17.3, 10.4 Hz, 1H), 5.84 (dd, *J* = 10.4, 1.4 Hz, 1H), 4.31 (dd, *J* = 5.5, 4.2 Hz, 2H), 4.28 (dd, *J* = 5.5, 4.1 Hz, 2H), 3.78 – 3.73 (m, 2H), 3.73 – 3.69 (m, 2H), 3.69 – 3.62 (m, 8H), 2.96 (t, *J* = 7.1 Hz, 2H), 2.84 (s, 4H), 2.78 (t, *J* = 7.0 Hz, 2H); ^{13}C NMR (101 MHz, $CDCl_3$) δ 176.31, 172.06, 166.21, 131.08, 128.25, 70.70, 70.53, 70.46, 69.09, 68.99, 63.86, 63.63, 29.16, 28.97. HRMS (ESI) Calcd for C15H25O9 [M+H]+ : 349.1494, found 349.1495.

^{1}H NMR spectrum (400 MHz, $CDCl_3$) of compound 2

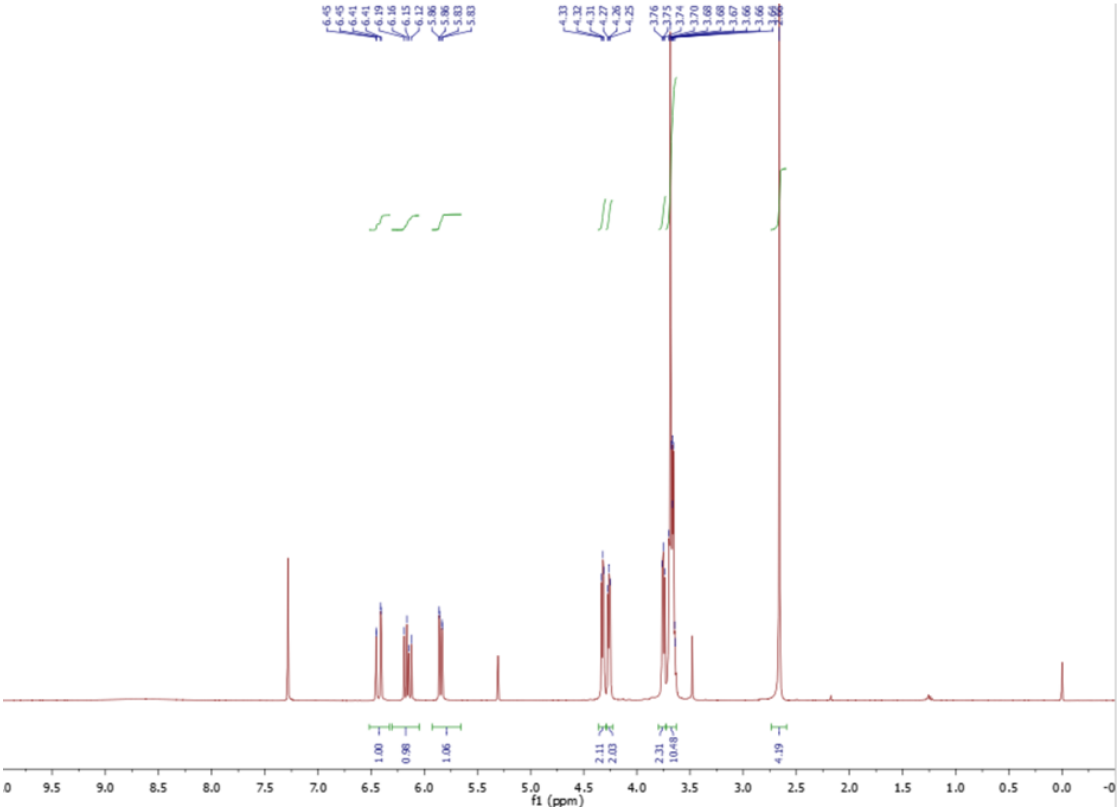

^{13}C NMR spectrum (101 MHz, $CDCl_3$) of compound 2

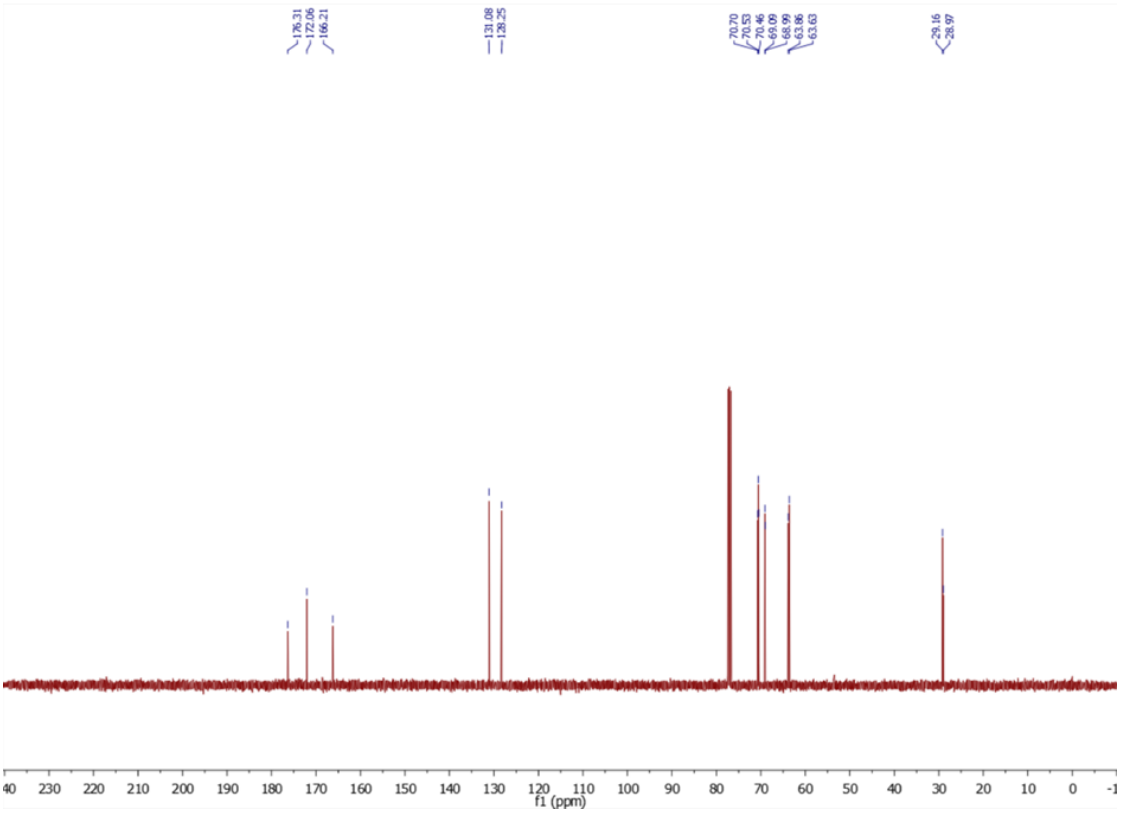

2,5-dioxopyrrolidin-1-yl (13-oxo-3,6,9,12-tetraoxapentadec-14-en-1-yl) succinate (3)

To a RBF with a stirring bar, **2** (5.7 mmol, 2 g) and NHS (6.3 mmol, 0.73 g) were added to 40 mL anhydrous DCM under nitrogen atmosphere. The mixture was stirred at 0 ºC for 30 min. then EDC (6.3 mmol, 0.98 g) in DCM was added to the solution dropwise. The reaction was stirred at r.t. overnight. After that, the solution was washed with brine. The product was extracted with DCM. The solvent was removed using rotary evaporation and purified by column chromatography (silica gel, EA). The final product was isolated as a colorless oil (1.9 g, 75 %). ^{1}H NMR (400 MHz, $CDCl_3$) δ 6.43 (dd, *J* = 17.3, 1.3 Hz, 1H), 6.15 (dd, *J* = 17.3, 10.4 Hz, 1H), 5.85 (dd, *J* = 10.4, 1.3 Hz, 1H), 4.36 – 4.29 (m, 2H), 4.29 – 4.23 (m, 2H), 3.80 – 3.73 (m, 2H), 3.73 – 3.63 (m, 10H), 2.66 (s, 4H); ^{13}C NMR (101 MHz, $CDCl_3$) δ 170.97, 168.90, 167.69, 166.16, 131.01, 128.29, 70.62, 70.58, 69.12, 68.94, 64.18, 63.68, 28.67, 26.27, 25.57. HRMS (ESI) Calcd for C19H28NO11 [M+H]+ : 446.1657, found 446.1647.

^{1}H NMR spectrum (400 MHz, $CDCl_3$) of compound 3

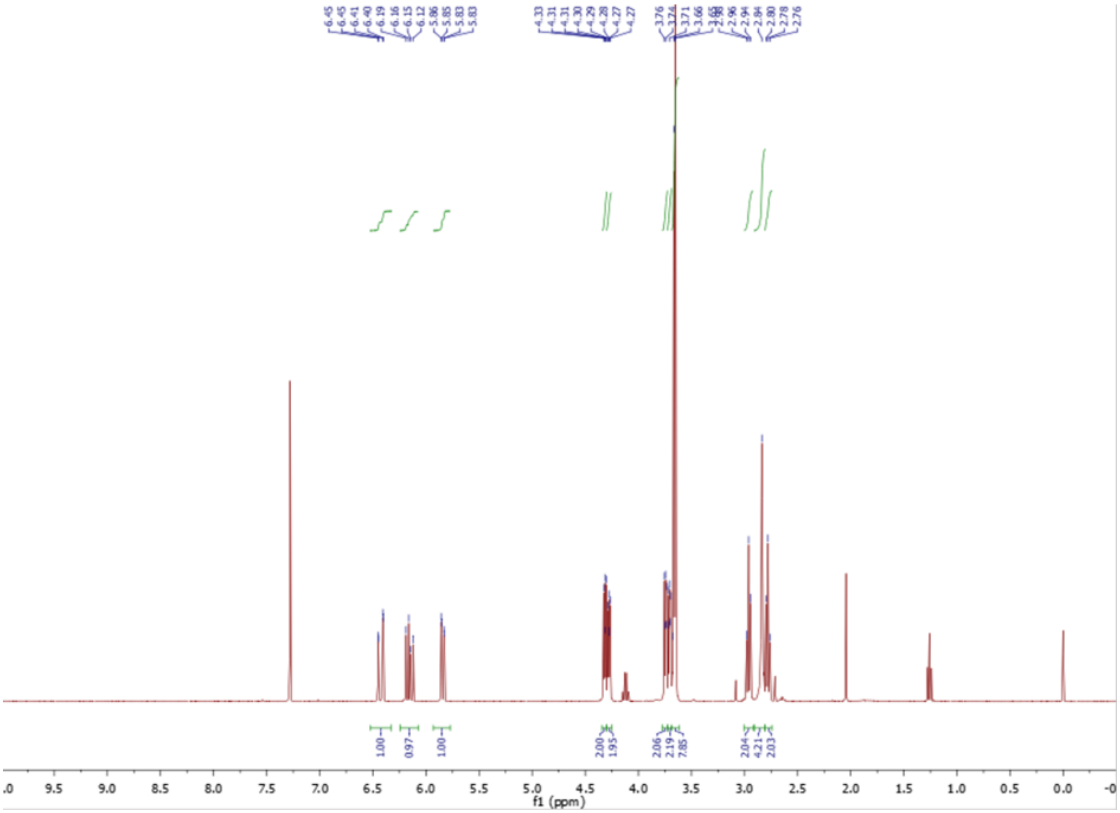

^{13}C NMR spectrum (101 MHz, $CDCl_3$) of compound 3

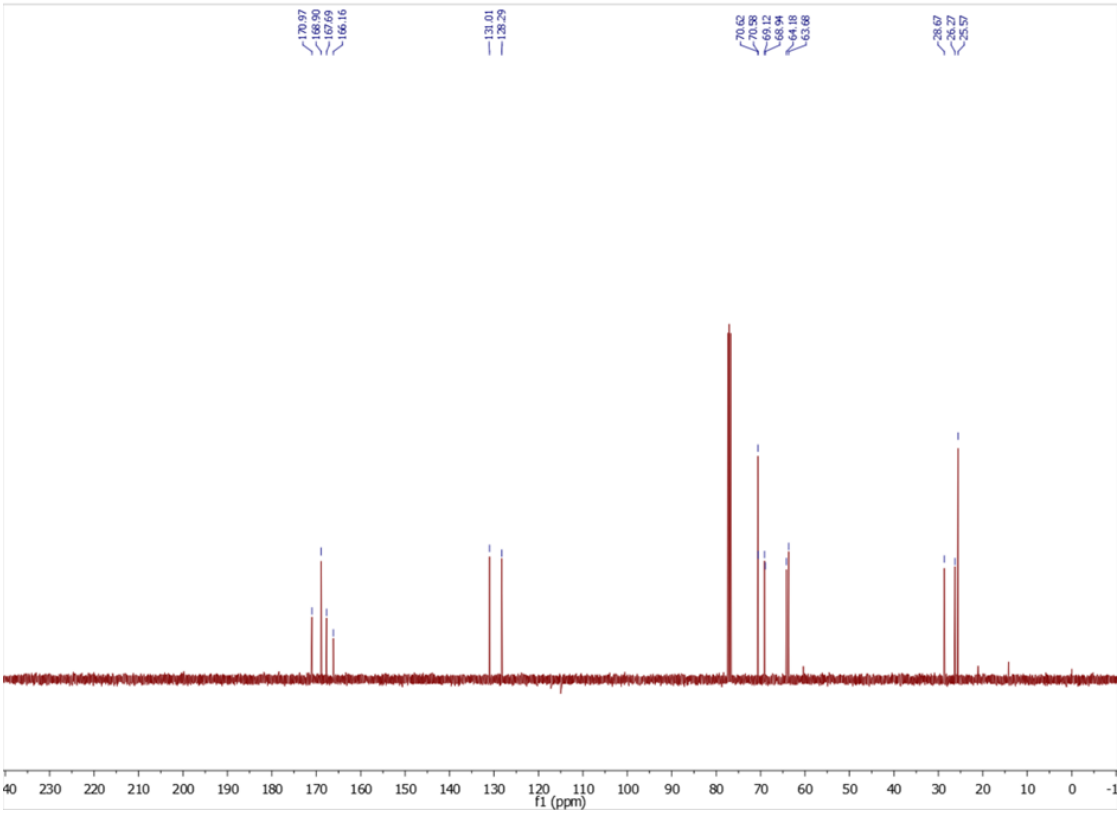

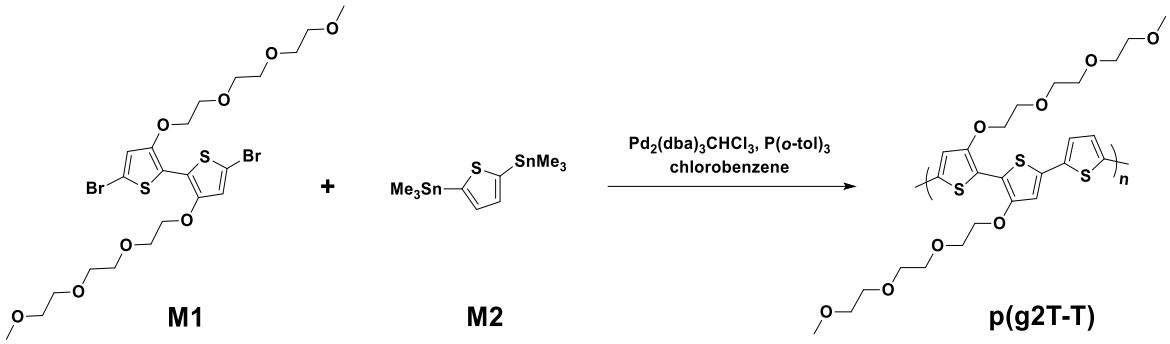

To a mixture of 5,5'-dibromo-3,3'-bis(2-(2-(2-methoxyethoxy)ethoxy)ethoxy)-2,2'-bithiophene (**M1**, 100 mg, 0.155 mmol, 1.0 eq.), 2,5-bis(trimethylstannyl)thiophene (**M2**, 63.8 mg, 0.155 mmol, 1.0 eq.), $Pd_2(dba)_3$ $CHCl_3$ (3.2 mg, 0.0031 mmol, 0.02 eq.), and P(*o*-tol)$_3$ (3.8 mg, 0.0124 mmol, 0.08 eq.) was added 2 mL of chlorobenzene in a nitrogen-filled glovebox. The reaction vial was sealed and submitted to a microwave reactor with the following temperature profile: 2 minutes at 80 °C and 5 minutes at 100 °C. After the reaction was cooled down, 10 mol% of trimethyl(phenyl)stannane were added and the crude polymer solution was heated again to 2 minutes at 80 °C. To complete the end-capping of the polymer, 10 mol% of bromobenzene were added and the reaction vessel was submitted one last time to microwave heating (2 minutes at 80 °C). The crude polymer was then precipitated into methanol, filtered, loaded to a Soxhlet thimble and washed successively with hexane, acetone (each for 24 h). The polymer was finally collected from the thimble with chloroform. The solvent was then removed using rotary evaporation and the polymer was obtained as a blue solid.

^{1}H NMR spectrum (400 MHz, $CDCl_3$) of polymer p(g2T-T)

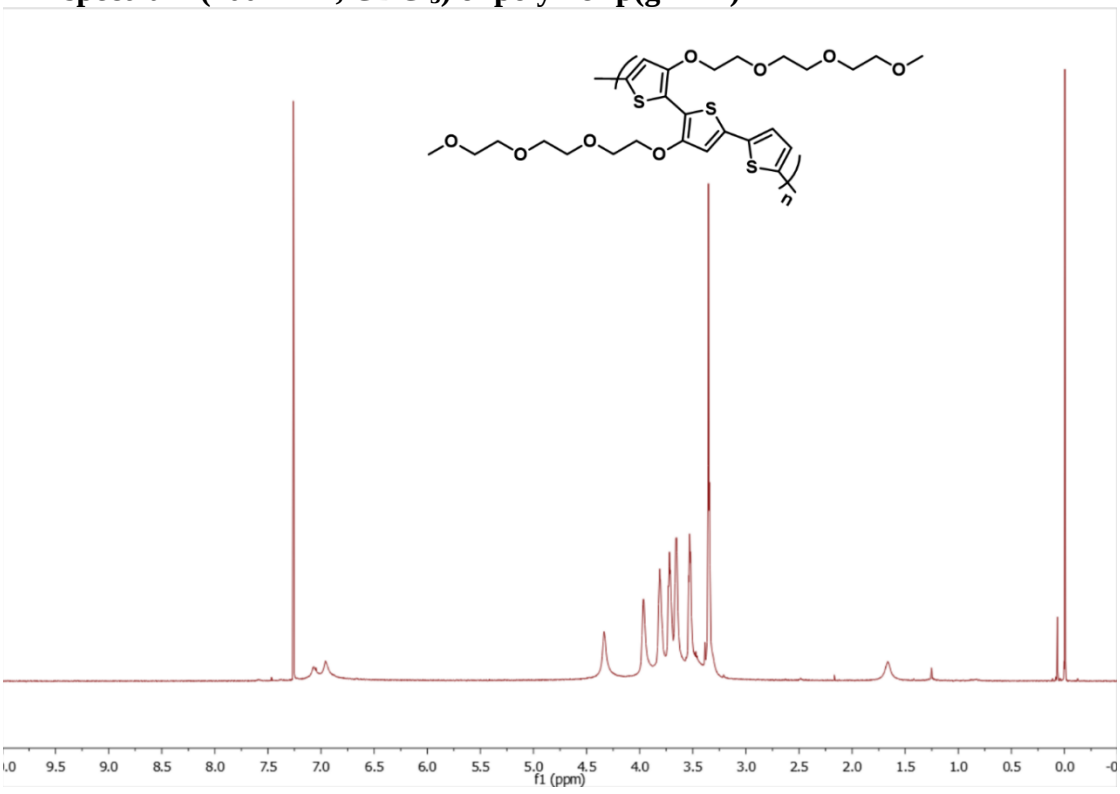

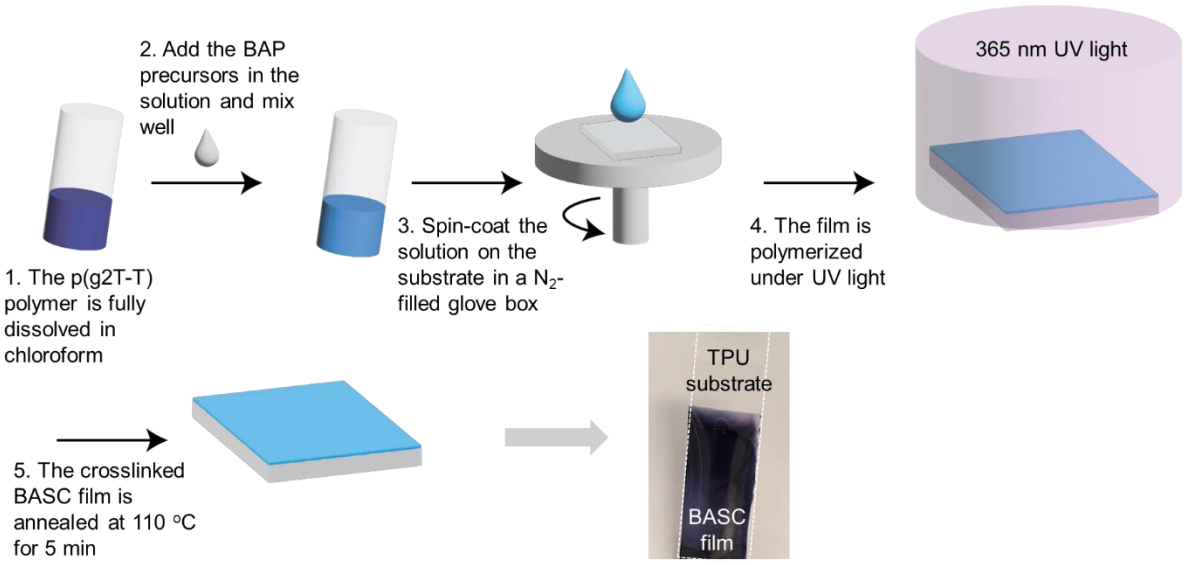

Fig. S1. **Schematic diagram illustrating the preparation of the BASC film.** 1. The semiconducting polymer p(g2T-T) is dissolved in chloroform under stirring at 60 °C. 2. The BAP precursor solution including the corresponding amount of adhesive monomers, crosslinker, and photoinitiator in chloroform is added to the p(g2T-T) solution and mix well under stirring. 3. The solution is spin-coated on the substrate (for example, OTS substrate, TPU) in a nitrogen gas-filled glovebox. 4. The film is subject to 365 nm UV light for 5 min to polymerize the adhesive network in a nitrogen gas-filled glovebox. 5. The crosslinked film is annealed at 110 °C for 5 min to complete the BASC film preparation in the glovebox. The typical film thickness is a few micrometers.

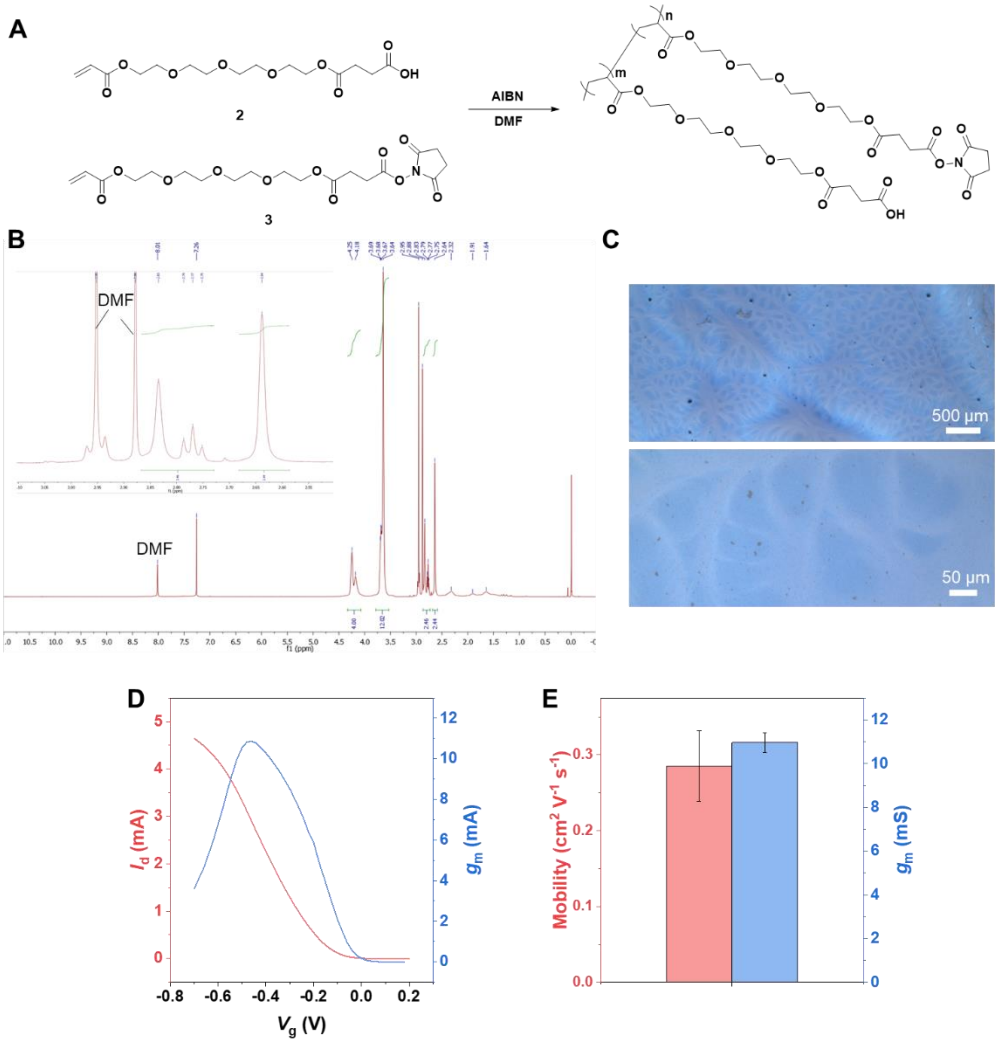

Fig. S2. Comparison of blending with pre-polymerized BAP poly(COOH-*co*-NHS), which displays large-scale phase separation. (**A**) Polymerization reaction through reversible addition-fragmentation chain transfer polymerization. Specifically, ACTEGNHS monomer (0.224mmol), ACTEGCOOH monomer (0.286 mmol), AIBN (0.0021 mmol), and ethyl 2-(phenylcarbonothioylthio)-2-phenylacetate (0.0051mmol, chain transfer agent) were dissolved in 2 mL anhydrous DMF in a Schlenk flask. The solution was freeze-pump-thaw for three cycles and heated at 70 °C for 12 hours. After the reaction, the mixture was precipitated in diethyl ether three times and the polymer was collected and vacuum-dried overnight to afford a yellow solid (40 % yield). The polymer shows a M_n of 43 kDa and a M_w of 89 kDa measured from GPC using DMF + 0.01 M LiBr as eluent (50 ºC) calibrated with PMMA standards. (**B**) ^{1}H NMR spectrum of the poly(COOH-*co*-NHS). (**C**) Microscopic images of the blended film with a weight ratio of p(g2T-T) to poly(COOH-*co*-NHS) equaling 1-40. The film was spin-coated on the silicon substrate and annealed at 110 ºC for 5 min. The blended film displays large phase separation between the two phases with large segregation of blue domains. (**D**) Transfer curves from the OECT measurement for such a blended film. (**E**) Charge-carrier mobility (determined from constant gate current method) and g_m for the blended film. Values represent the mean and the standard deviation (n = 5).

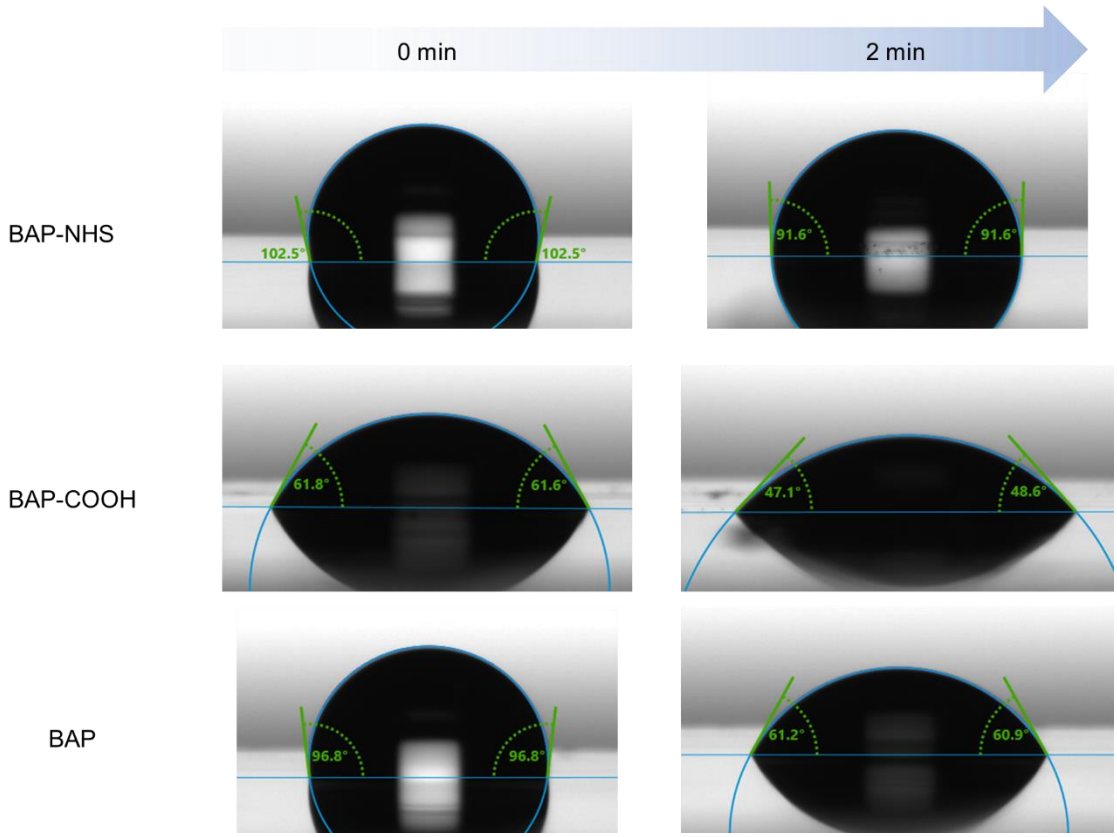

Fig. S3. **Photographs showing the changes of water wettability on the three types of bioadhesive polymer films over 2 min.** These films were prepared by spin-coating the precursors solution on OTS-treated glass substrates followed by photo-polymerization under 365 nm UV light for 5 min, and finally by annealing at 110 ^{o}C for 5 min in a nitrogen gas-filled glovebox.

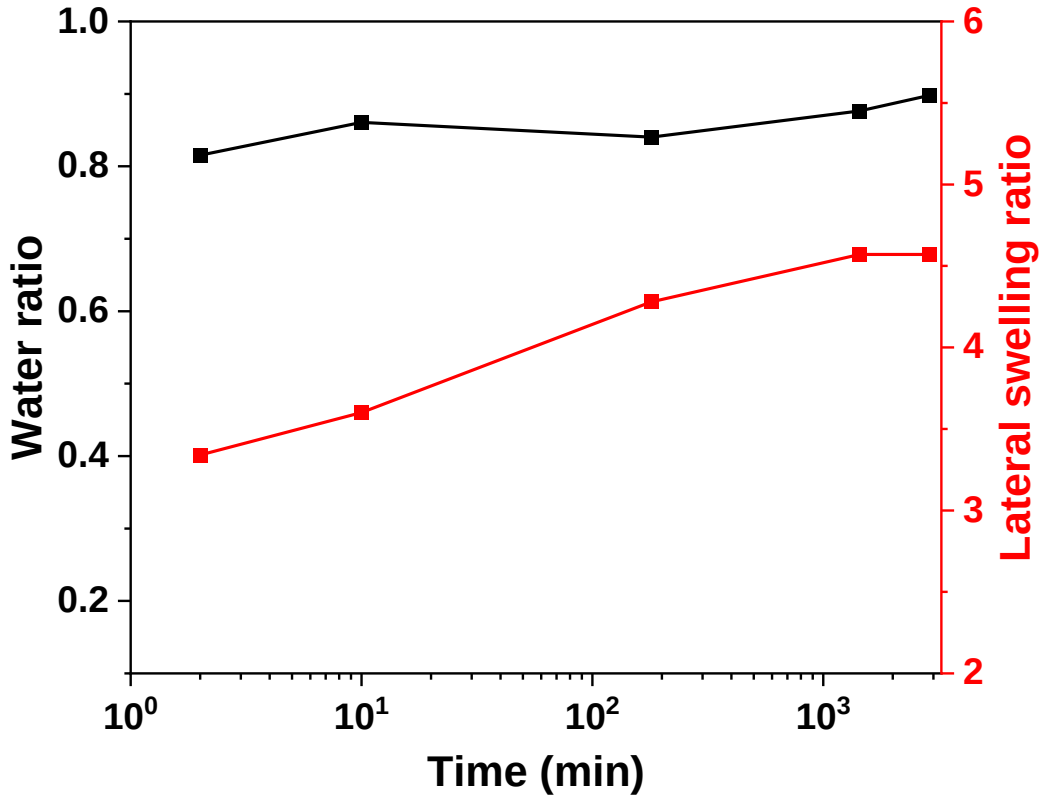

Fig. S4. Water absorption ratio and lateral swelling behavior of poly(acrylic acid) in PBS solution over time.

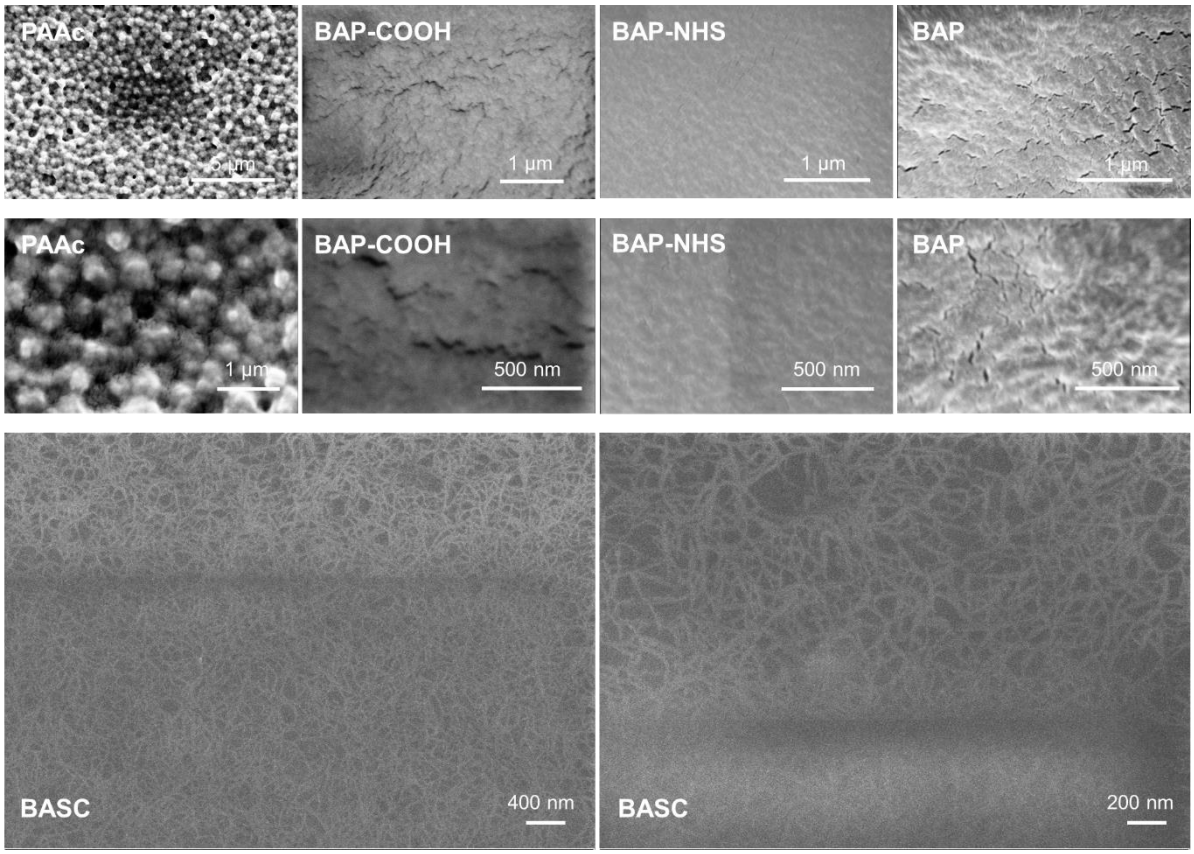

Fig. S5. SEM images of four types of bioadhesive polymer films (including PAAc, BAP-COOH, BAP-NHS, and BAP) and a BASC film in the dry state.

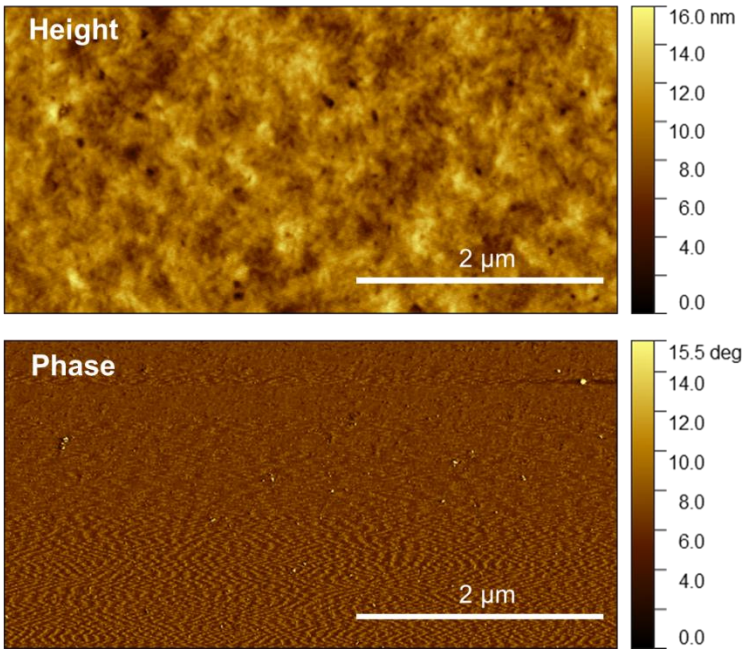

Fig. S6. AFM height and phase images of the neat p(g2T-T) film.

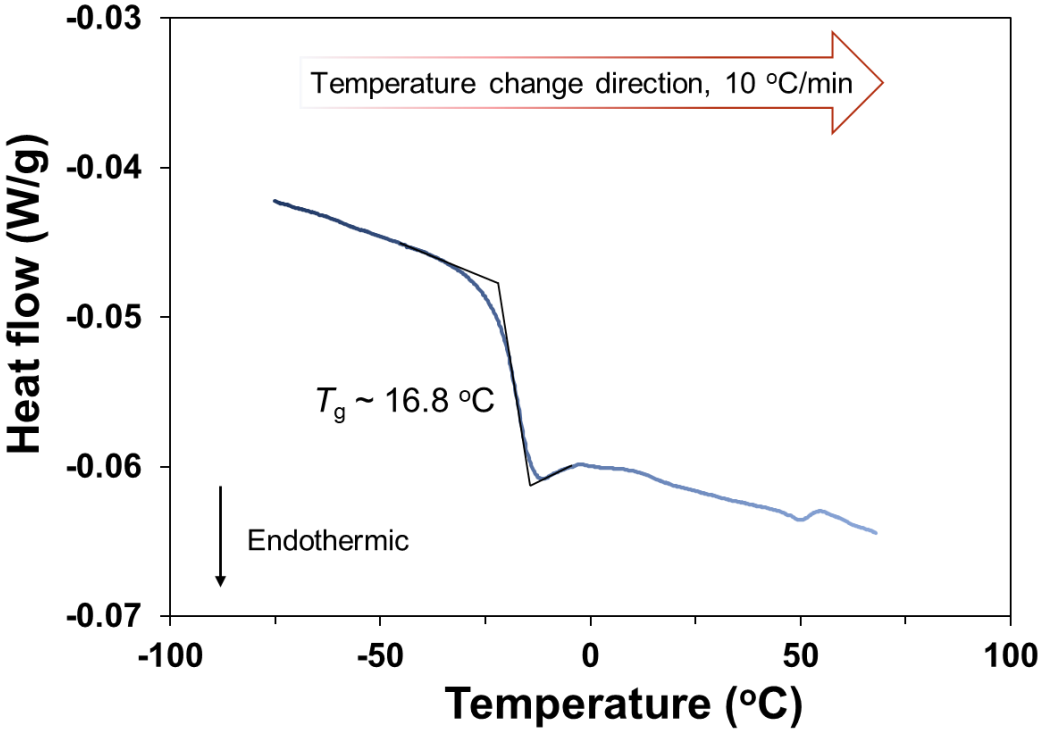

Fig. S7. Differential scanning calorimetry (DSC) thermal analysis of our BAP.

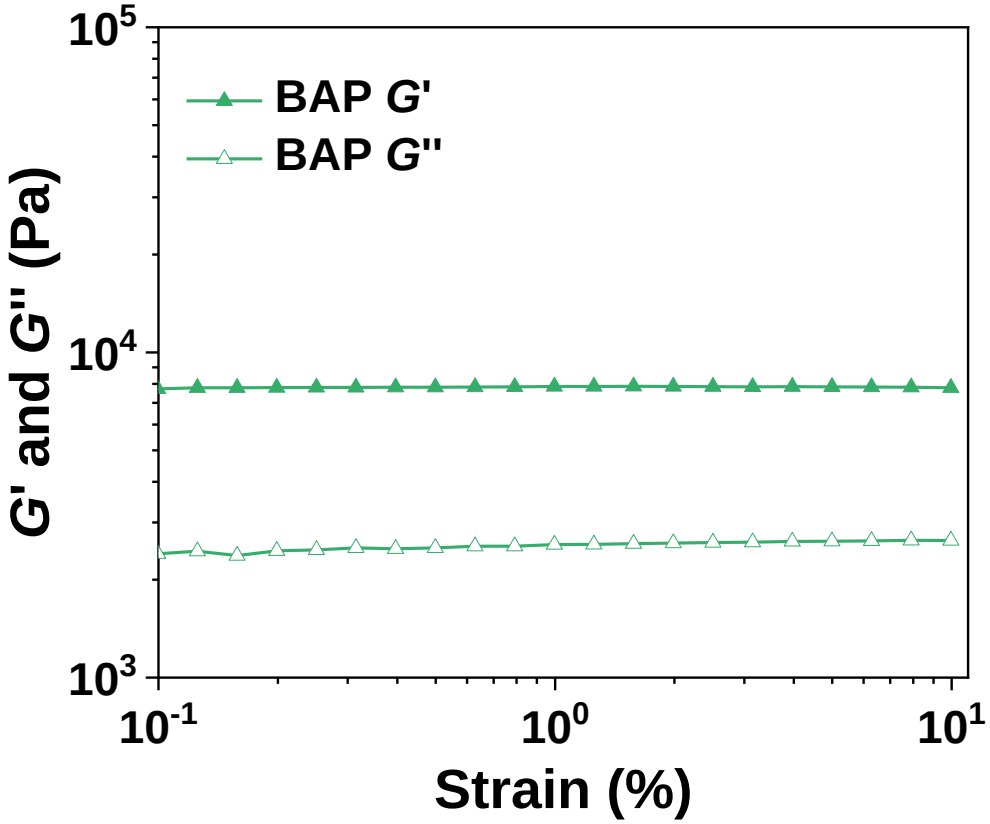

Fig. S8. Rheological measurement of our BAP in the dry state by performing amplitude sweep at 1 Hz with results showing storage modulus (*G*') and loss modulus (*G*'').

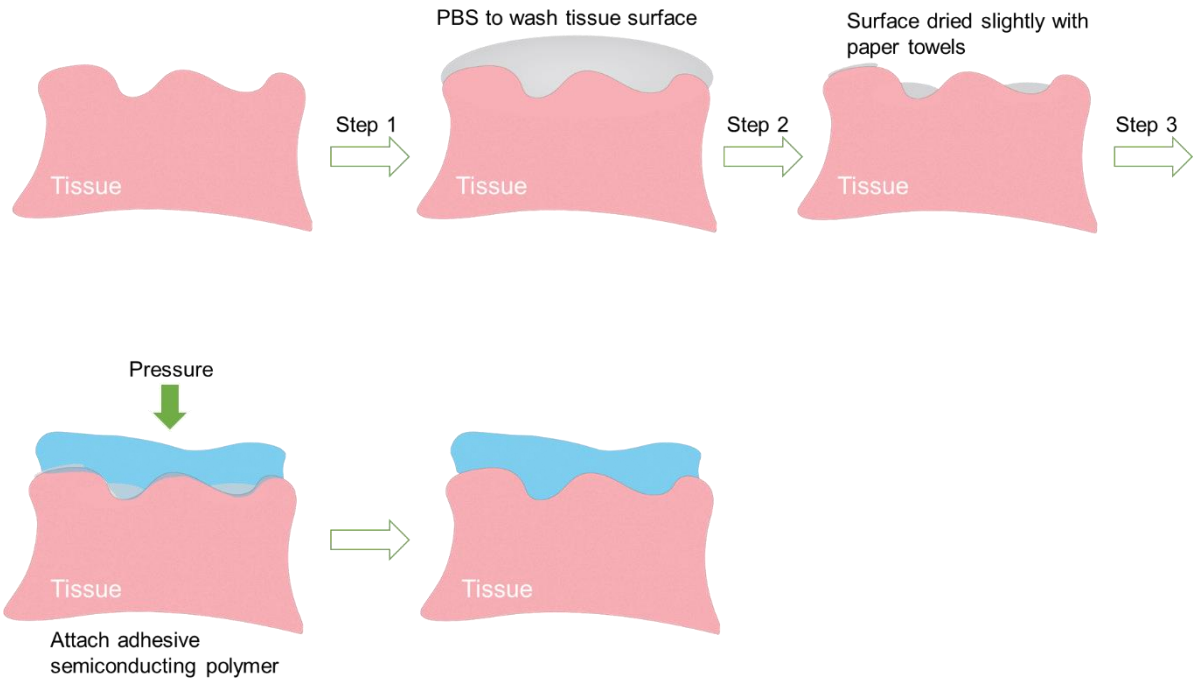

Fig. S9. Application process of the adhesive semiconducting polymer on wet tissue surfaces. Step 1, the tissue surfaces are gently washed with PBS solution to remove any debris and neutralize the surface. Step 2, the majority amount of solution is removed by paper towels to slightly dry the surface. Step 3, the BASC film (and controls) on a TPU substrate is applied to the tissue surface and gentle pressure is applied on the back side and is held for 1 min.

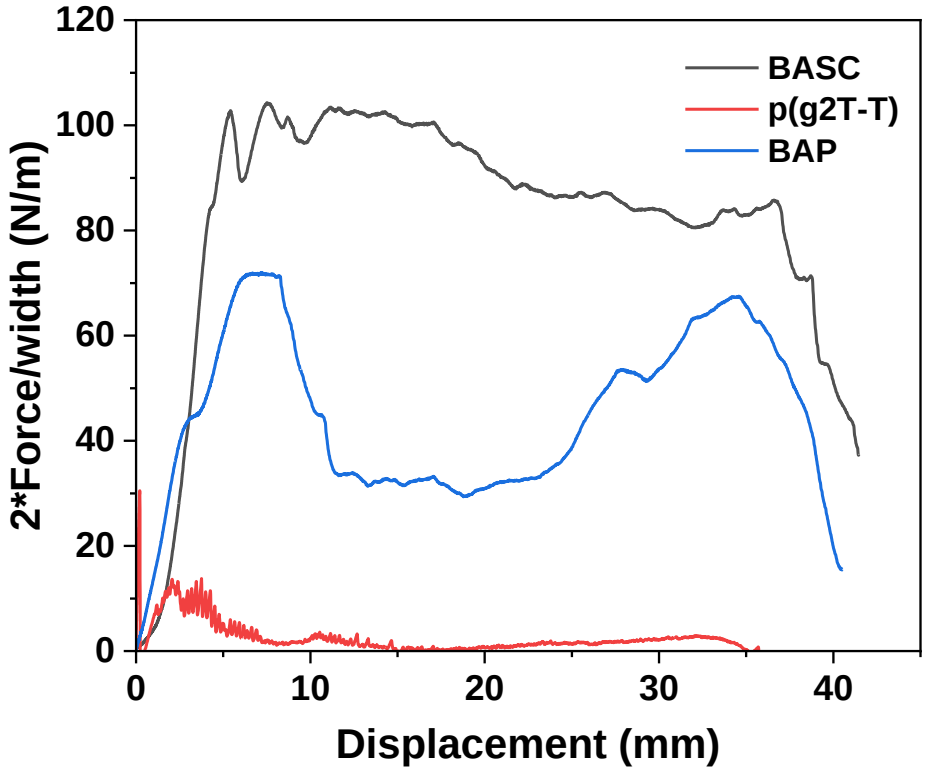

Fig. S10. 180°-peel tests of the adhesion of BASC, BAP, and p(g2T-T) films on amine-treated glass. For the adhesion tests, adhered samples with a width of 25 mm were prepared and tested by the 180-degree peel tests (ASTM D3330) for rigid substrates.

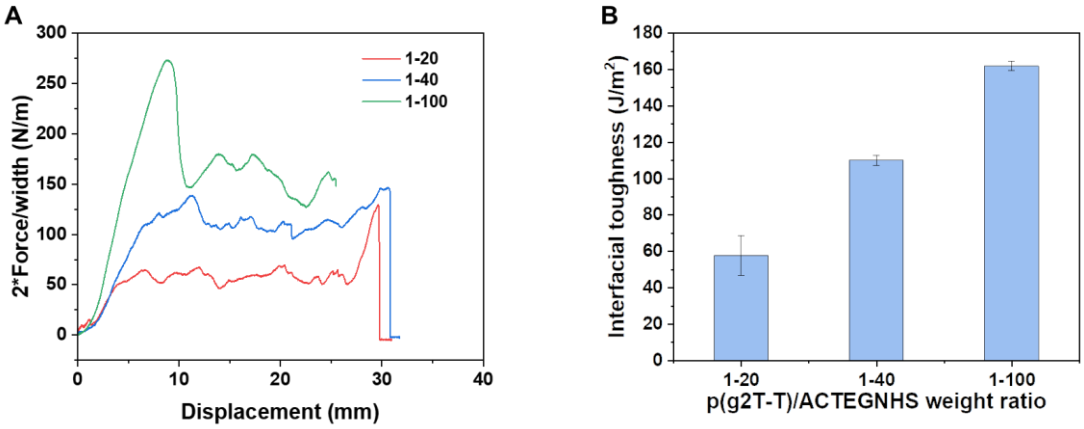

Fig. S11. 180°-peel tests of the adhesion of BASC-NHS films with different blending ratios on amine-treated glasses. (A) 2×Force/width vs displacement curves. **(B)** Interfacial toughness. For the adhesion tests, the TPU substrates were cut into a rectangular shape with a length/width of 80 mm/6 mm. The semiconducting polymer occupies one end with an average length/width of 10 mm/6 mm.

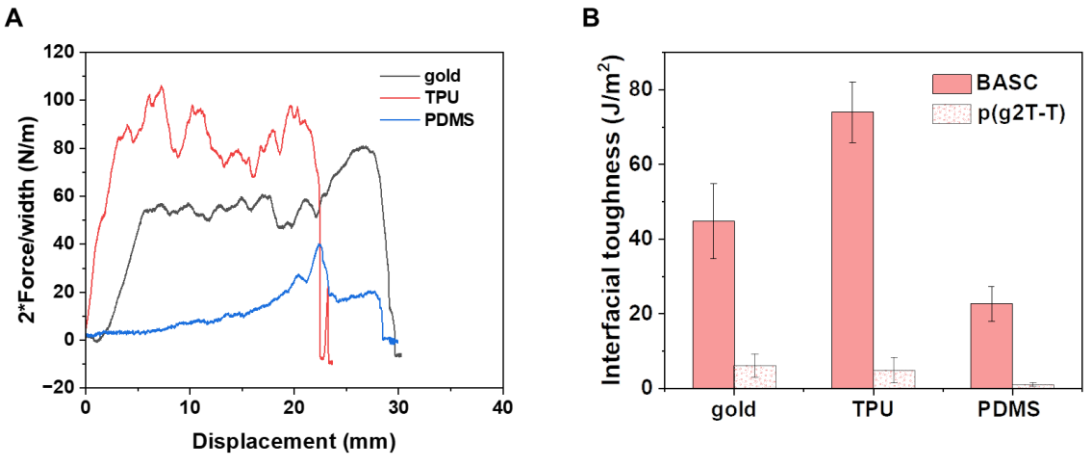

Fig. S12. 180°-peel tests of the adhesion performances of BASC films on other synthetic surfaces. (**A**) 2×Force/width vs. displacement curves for 180°-peel test of the BASC on different synthetic materials. (**B**) The interfacial toughness of the adhesion of BASC on different synthetic materials. For the adhesion tests, the TPU substrates were cut into a rectangular shape with a length/width of 80 mm/6 mm. The semiconducting polymer occupies one end with an average length/width of 10 mm/6 mm.

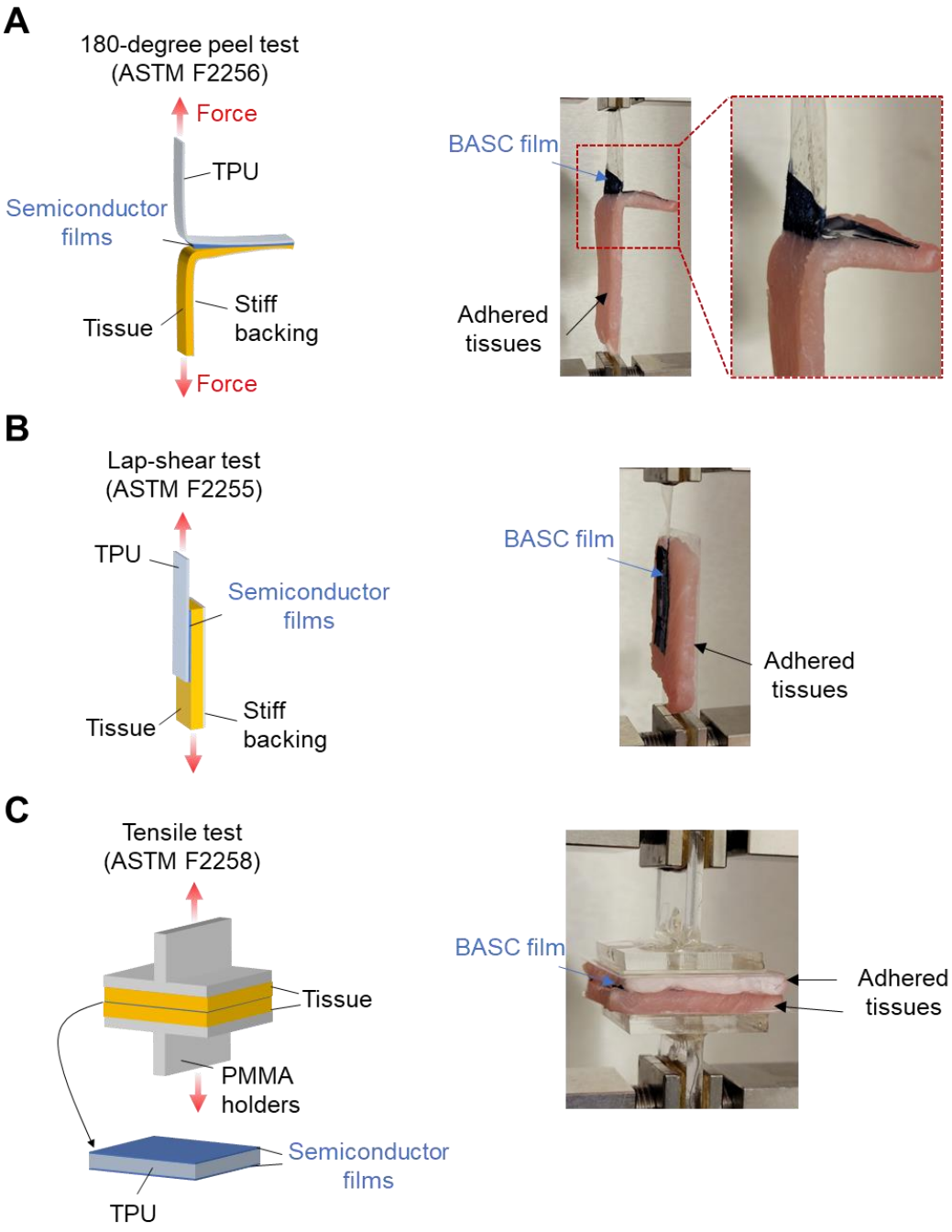

Fig. S13. Experimental setups for mechanical test of adhesion performance on bio-tissues. (**A**) 180-degree peel test (ASTM F2256) for interfacial toughness measurement. Adhered samples with a width of 25 mm were prepared. (**B**) Lap-shear test (ASTM F2255) for shear strength measurement. Adhered samples with an adhered area of 25 mm × 10 mm were prepared. (**C**) Tensile test (ASTM F2258) for tensile strength measurement. Adhered samples with an adhered area of 25 mm × 25 mm were prepared with double-side-coated adhesive semiconductor films. The adhesion test of BASC films on porcine muscles was illustrated on the right. Polyethylene terephthalate (PET) films were applied using Krazy Glue as a stiff backing for the bio-tissues.

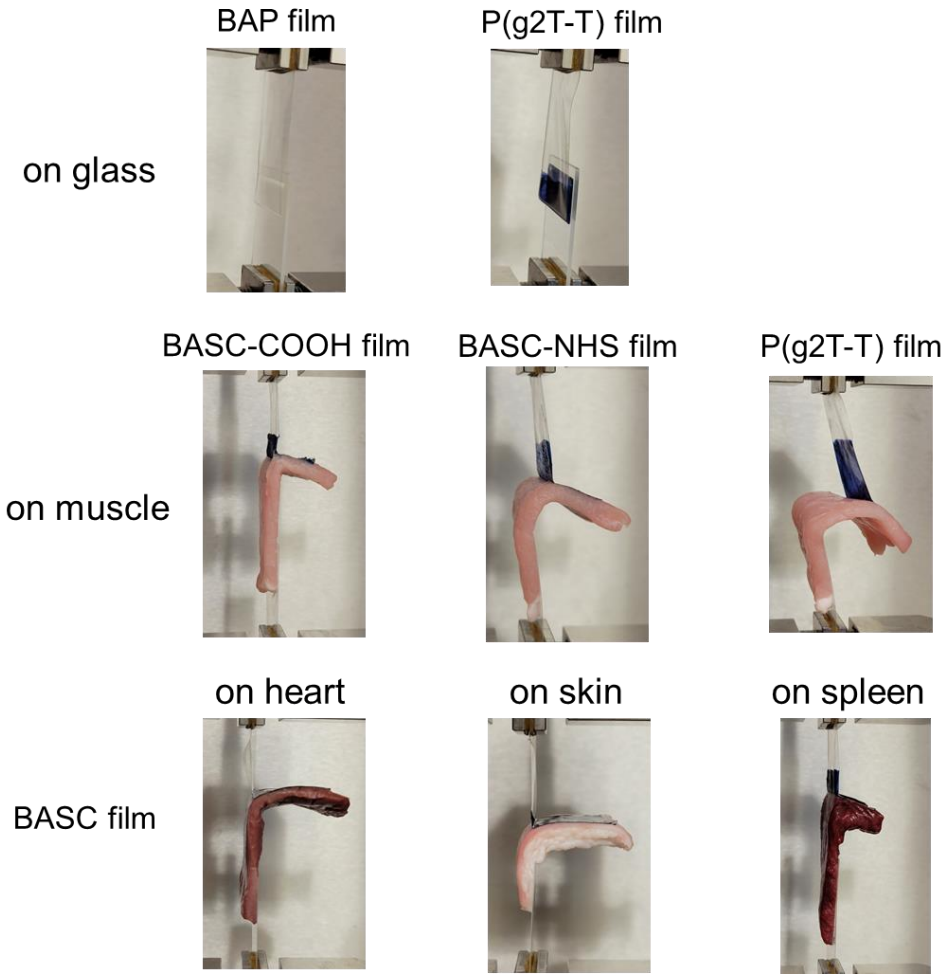

Fig. S14. Images of the adhesion test of different semiconducting films on the glass and bio-tissues.

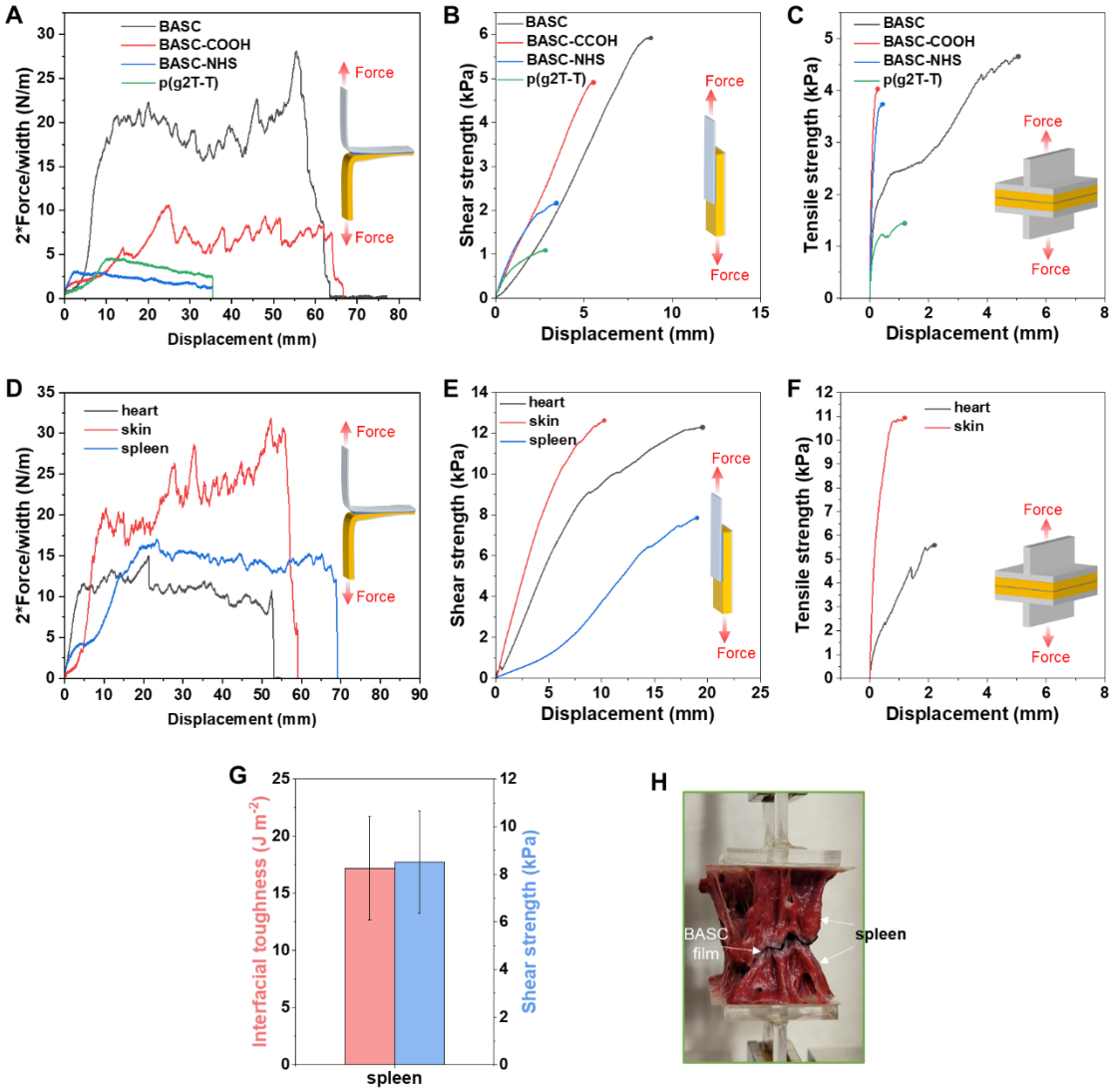

Fig. S15. Representative curves for the adhesion test of different polymer semiconductors on various bio-tissues. (**A**) 2×Force/width vs. displacement curves for 180°-peel test of different polymer semiconductors on porcine muscles. (**B**) Shear stress vs. displacement curves for lap-shear test of different polymer semiconductors on porcine muscles. (**C**) Tensile stress vs. displacement curves for tensile test of different polymer semiconductors on porcine muscles. (**D**) 2×Force/width vs. displacement curves for 180°-peel test of BASC on various bio-tissues. (**E**) Shear stress vs. displacement curves for lap-shear test of BASC on various bio-tissues. (**F**) Tensile stress vs. displacement curves for tensile test of BASC on various bio-tissues. (**G**) The interfacial toughness and shear strength of the adhesion of BASC on the porcine spleen. (**H**) An image of the tensile test of the adhesion of BASC on the porcine spleen. The spleen is too weak to get an accurate measurement of the tensile strength. For the interfacial toughness tests (ASTM F2256), adhered samples with a width of 25 mm were prepared. For the shear strength tests (ASTM F2255), adhered samples with an adhered area of 25 mm × 10 mm were prepared. For the tensile strength (ASTM F2258), adhered samples with an adhered area of 25 mm × 25 mm were prepared with double-side-coated adhesive semiconductor films.

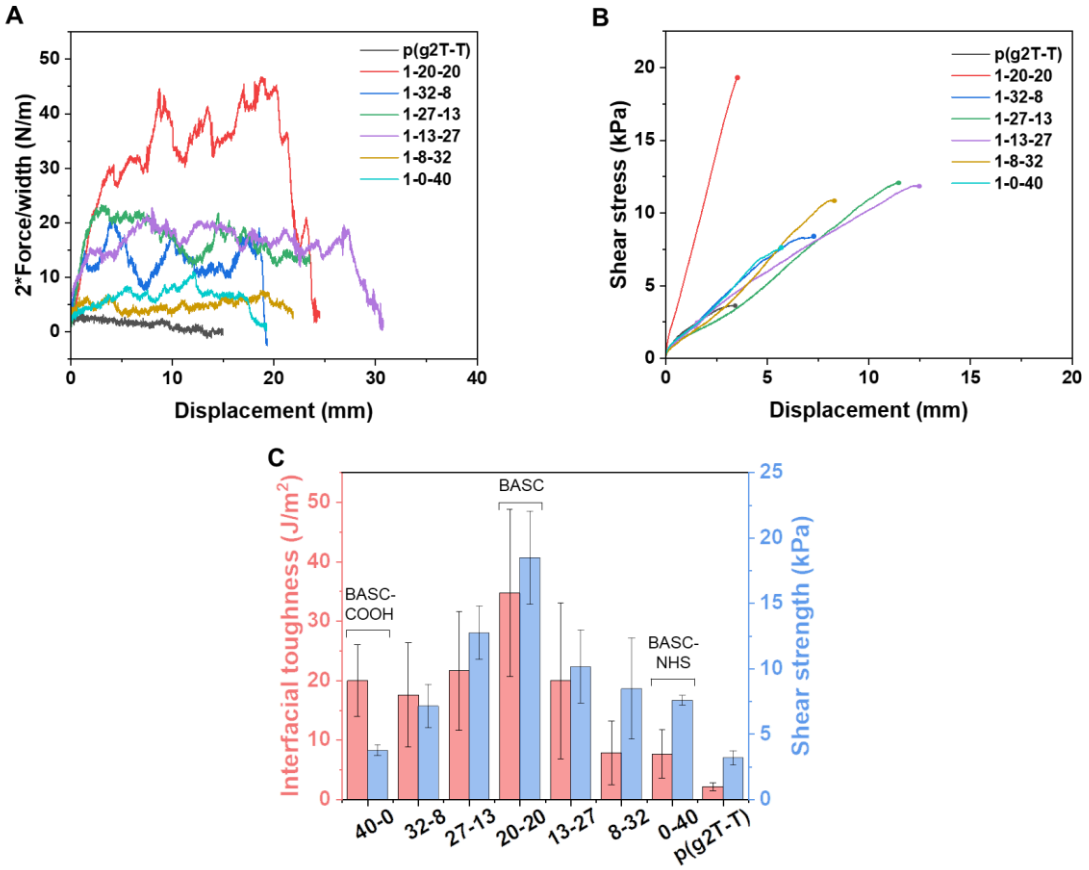

Fig. S16. 180°-peel tests and lap-shear tests of the adhesion on wet bio-tissues. (**A**) 2×Force/width vs. displacement curves, and (**B**) Shear stress vs. displacement curves of BASC films of different compositions on porcine muscles. (**C**) The interfacial toughness and shear strength of the adhesive semiconductors with different compositions on porcine muscles. For the adhesion tests, the TPU substrates were cut into a rectangular shape with a length/width of 80 mm/6 mm. The semiconducting polymer occupies one end with an average length/width of 10 mm/6 mm.

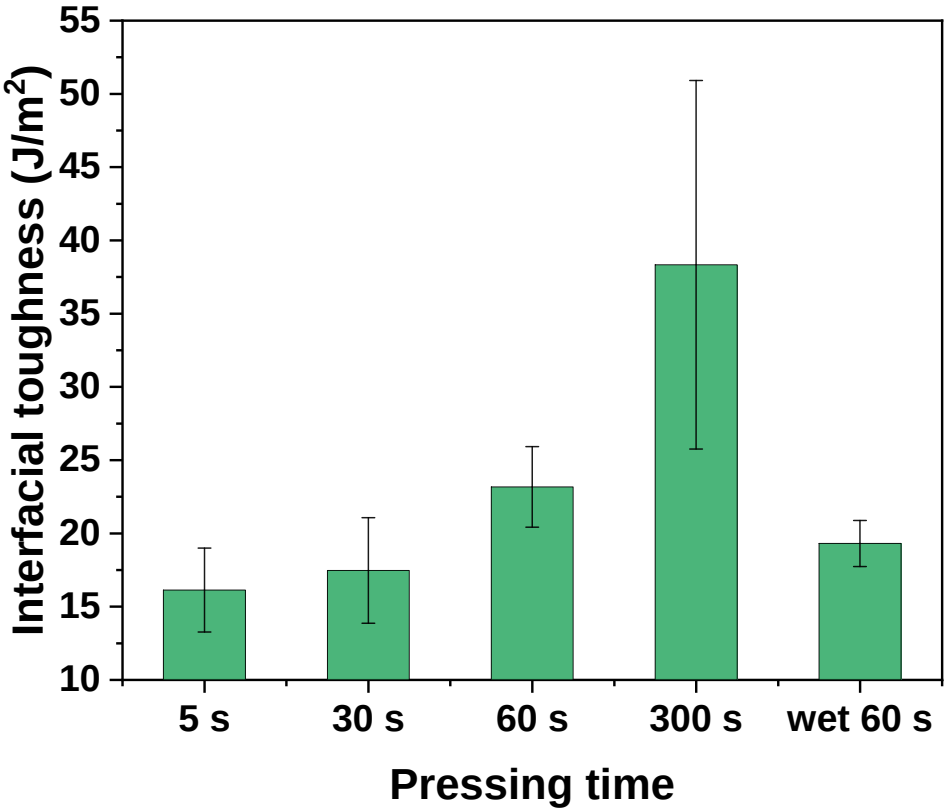

Fig. S17. Interfacial toughness of the BASC films on muscles with different pressing time and tissue hydration status. For comparing the pressing time, the BASC films were gently pressed (~5 kPa) on the slightly dried muscles with paper towels for different time scales from 5 s to 300 s. As a comparison of the tissue hydration status, copious amount of 0.1X PBS solution was sprayed on the tissue surface and a BASC film were directly applied on top and gently pressed for 60 s (this sample is labeled as "wet 60 s"). For the adhesion tests, the TPU substrates were cut into a rectangular shape with a length/width of 80 mm/6 mm. The semiconducting polymer occupies one end with an average length/width of 10 mm/6 mm.

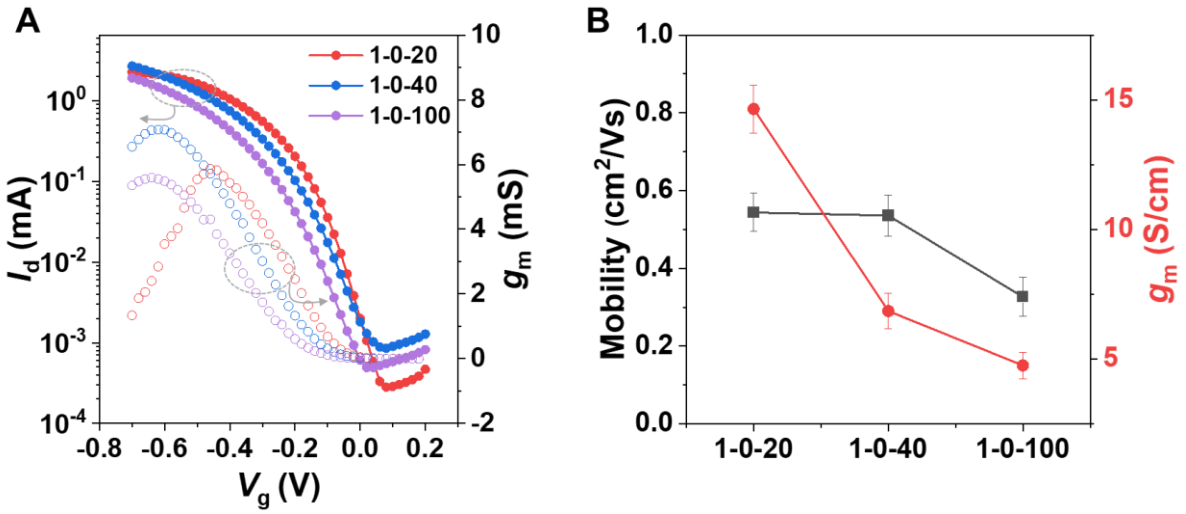

Fig. S18. OECT electrical performance for three types of BASC films with different compositions. (A) Transfer curves. **(B)** Mobility (obtained from the constant-gate-current method (*59*)) and transconductances.

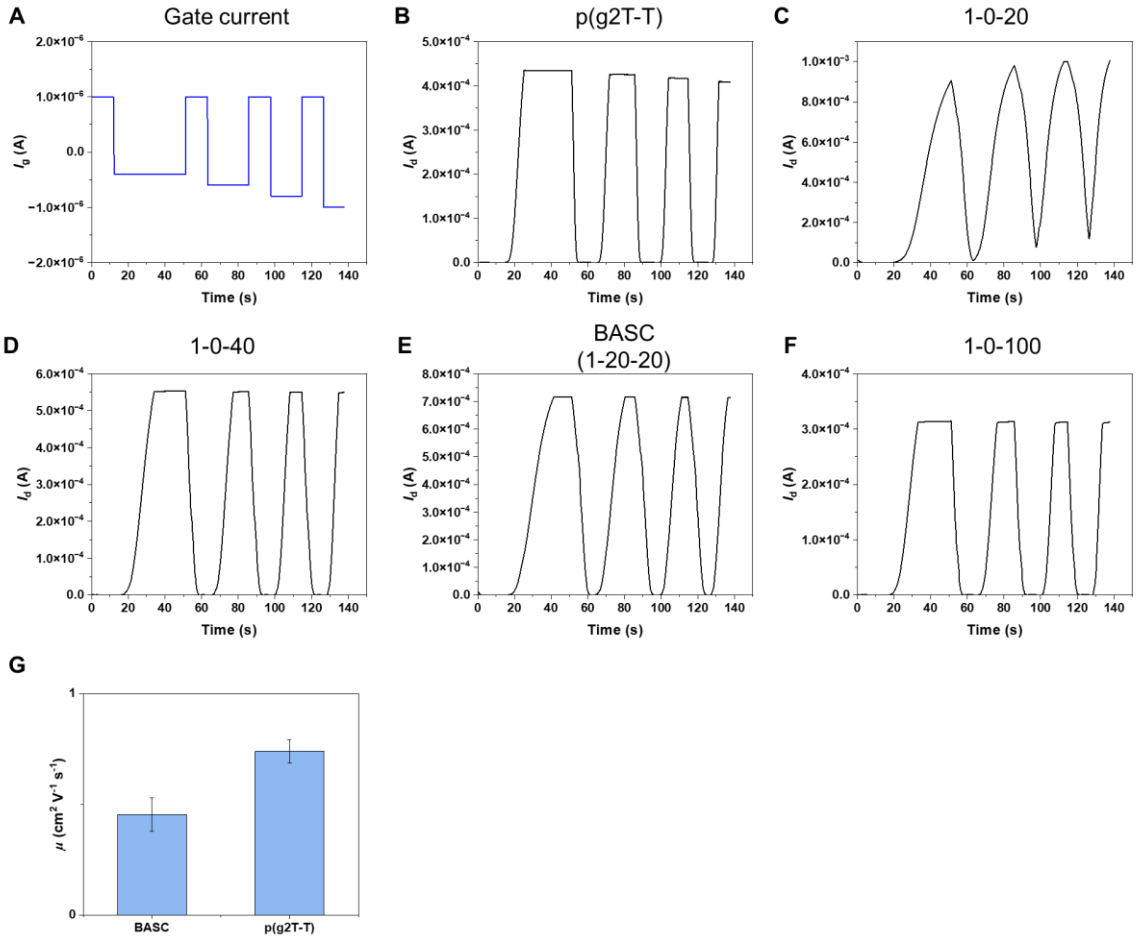

Fig. S19. Constant gate current method (*59*) for extracting the charge carrier mobility from OECTs. (**A**) Applied gate currents. (**B-F**) Absolute drain current responses for different semiconducting polymers, p(g2T-T) (**B**), 1-0-20 (**C**), 1-0-40 (**D**), BASC (1-20-20) (**E**), 1-0-100 (**F**). (**G**) Charge-carrier mobility for the BASC and p(g2T-T) films calculated from the constant gate current method.

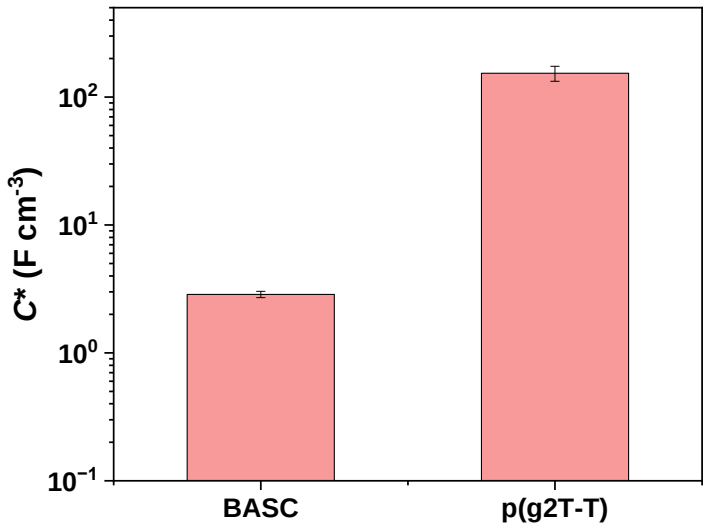

Fig. S20. Volumetric capacitance (*C) of the BASC and p(g2T-T) films.**

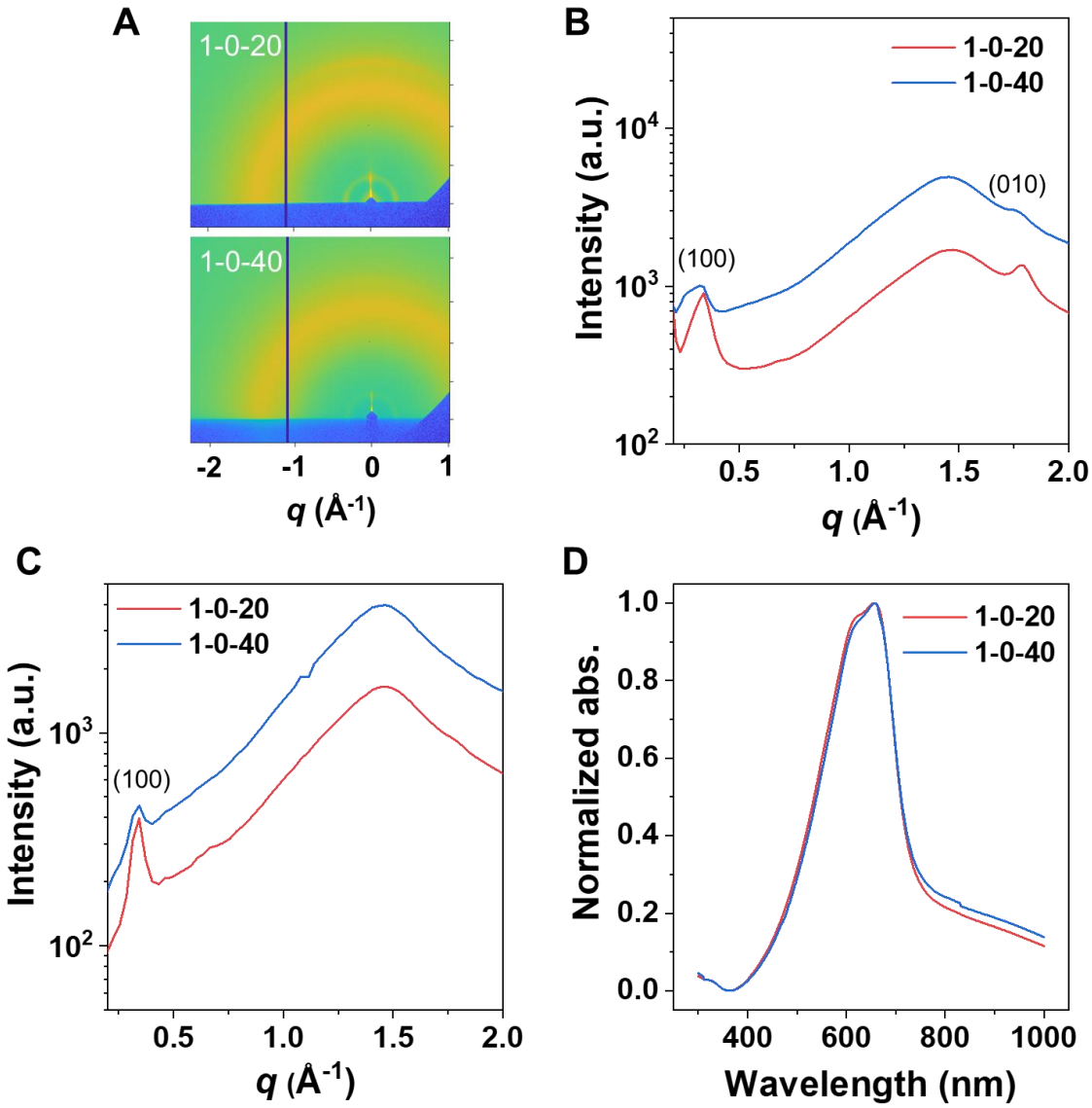

Fig. S21. Structural characterizations for BASC films of 1-0-20 and 1-0-40 compositions. (**A**) 2D GIXD patterns. (**B**) 1D linecuts for the out-of-plane direction. (**C**) 1D linecuts for the in-plane direction. (**D**) UV-vis spectra.

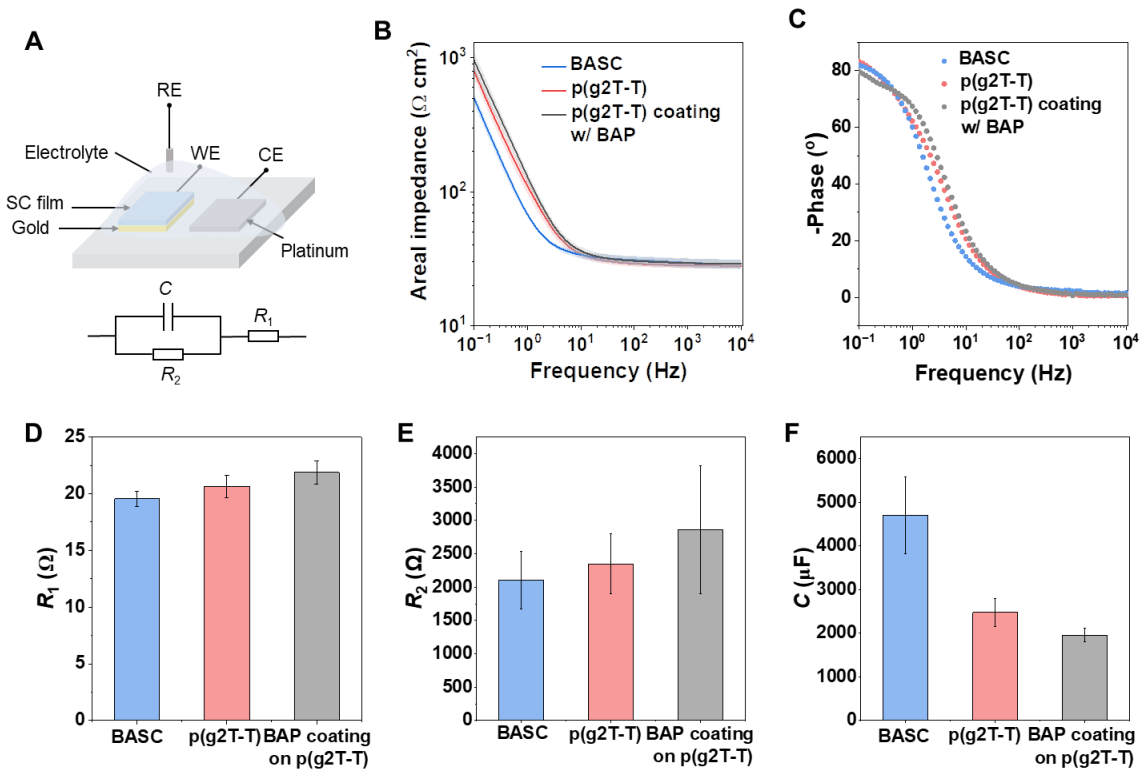

Fig. S22. EIS impedance measurement. (**A**) Schematic diagram showing the EIS measurement setup and the simplified Randles equivalent circuit diagram utilized for characterizing the surface impedances. The working electrode (WE) is semiconducting-film-coated gold; the counter electrode (CE) is platinum; the reference electrode (RE) is Ag/AgCl. The electrolyte is PBS solution. (**B**) Areal impedance of a BASC film, a p(g2T-T) film, and a bilayer p(g2T-T) film coated with a BAP layer (thickness of ~2.5 μm). (**C**) EIS phase spectrum. (**D**-**E**) EIS fitting parameters of the electrolyte resistance (**D**), charge transfer resistance (**E**), and capacitance (**F**).

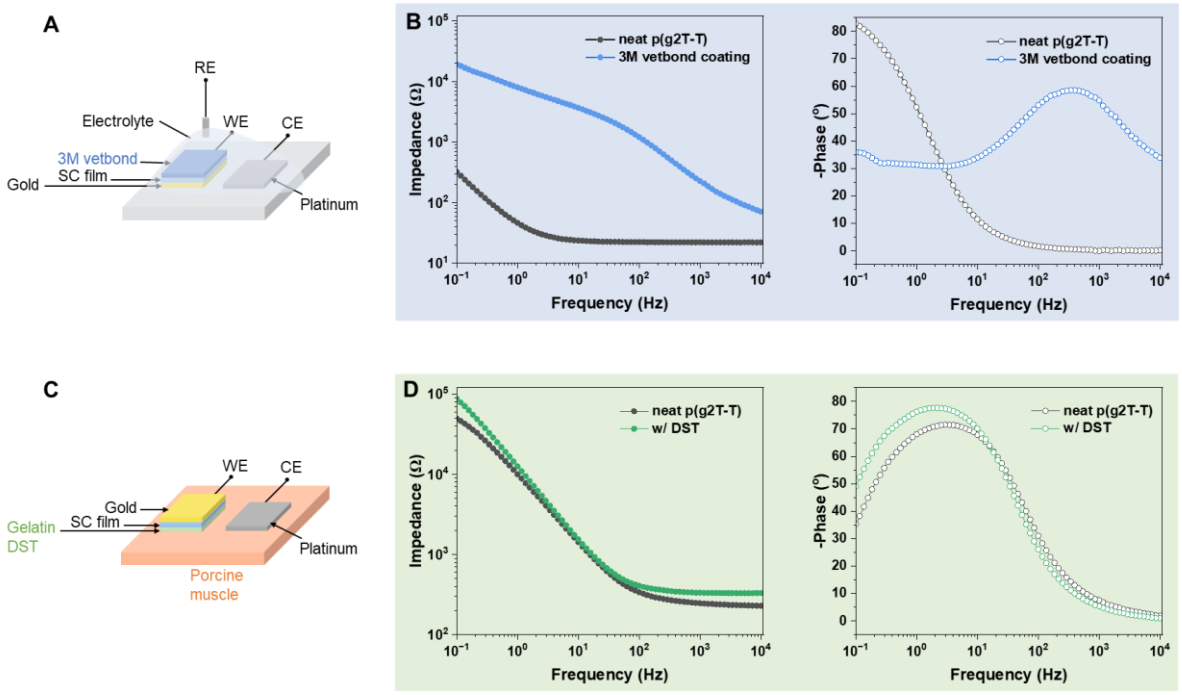

Fig. S23. Impedance comparison with state-of-the-art tissue adhesives. (**A**) EIS measurement setup for 3M vetbond tissue adhesive as a coating layer on p(g2T-T) film. The tissue adhesive was applied on p(g2T-T) film as a thin layer. Upon contact with water, the adhesive cures. The EIS measurement was done in PBS solution with a Pt counter electrode and an Ag/AgCl reference electrode. (**B**) Comparison of the EIS impedance and phase measurement results for 3M vetbond tissue adhesive coated on the p(g2T-T) film. (**C**) EIS measurement setup for gelatin-based double-sided tape (DST) as a coating layer on p(g2T-T) film. The measurements were carried out by attaching the WE (supported by an SEBS1052 substrate) and Pt CE to a wet porcine muscle. Specifically, the dry gelatin DST (made following the literature (*29*); dry thickness ~200 μm) was attached to the tissue surface and waited for the adhesive to hydrate. Then the semiconductor film was then attached to the top side of the DST layer. The reason for doing the impedance measurement on porcine muscle here is that attaching the dry gelatin DST on the p(g2T-T) film cannot guarantee conformable and stable contact, therefore performing such impedance measurement in PBS solution may not give very reliable results. (**D**) Comparison of the EIS impedance and phase measurement results for gelatin-based DST coated on the p(g2T-T) film.

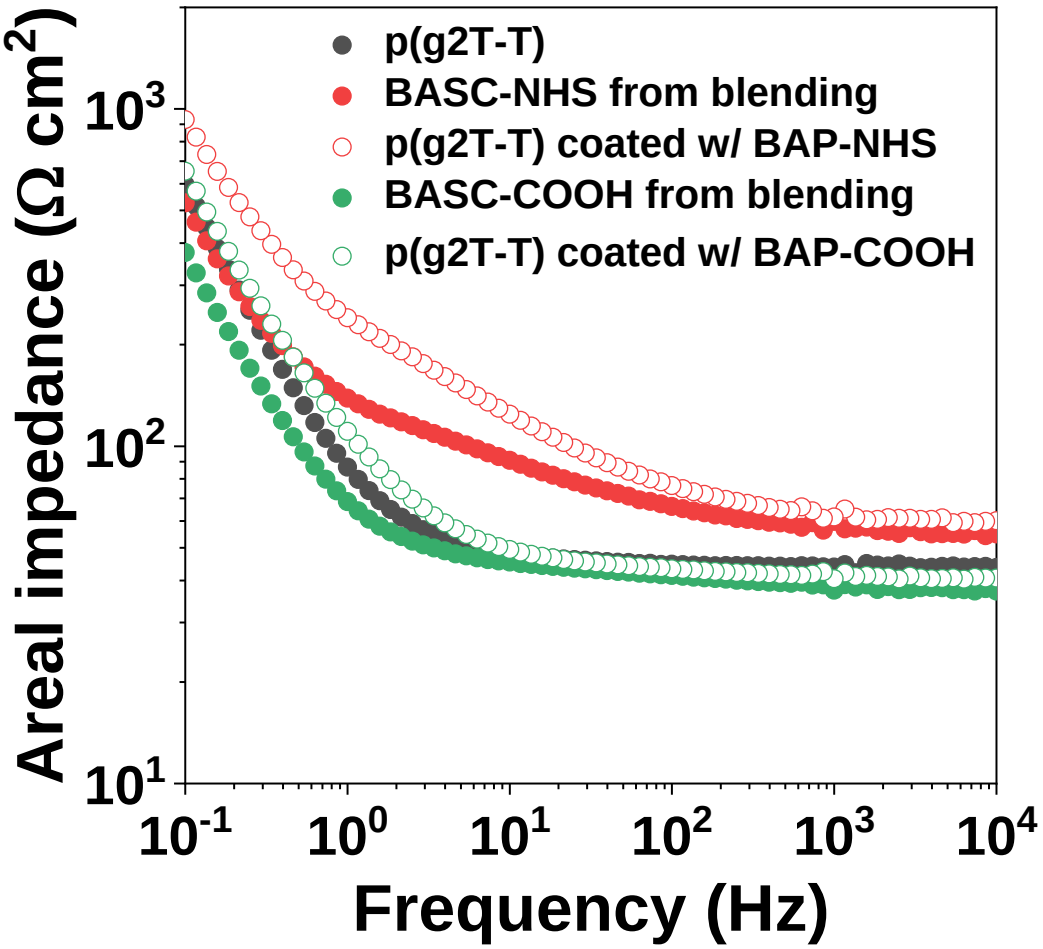

Fig. S24. EIS measurement of a neat p(g2T-T) film, two types of BASC films with the double-network design, and bilayer coating of two types of BAP on the surfaces. The comparisons of BASC-NHS and BASC-COOH films further illustrate the importance of the side-chain's hydrophilicity in BAP for decreasing the interfacial impedance.

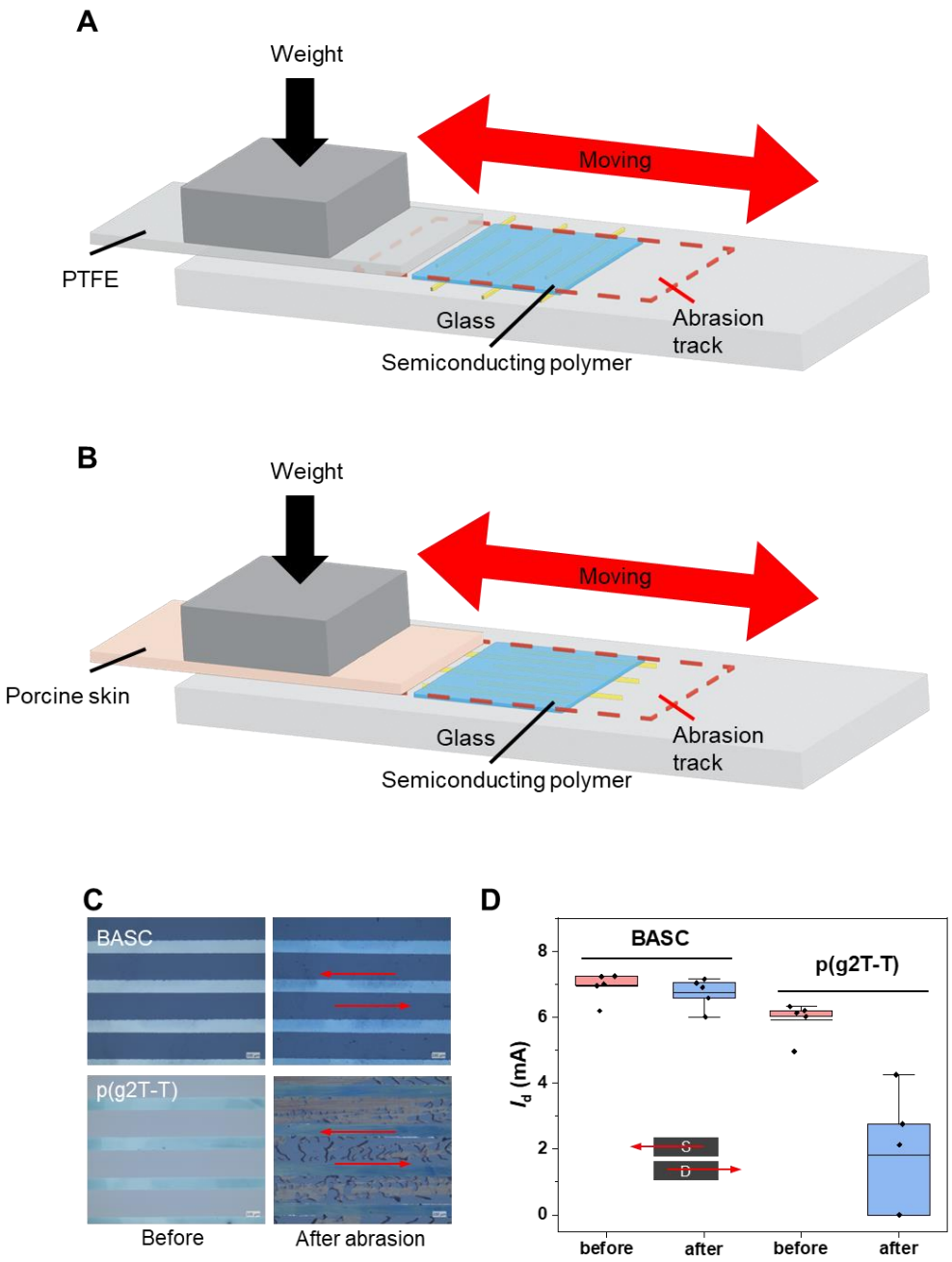

Fig. S25. Anti-abrasion property of the semiconductors. (**A**) Schematic diagram showing the abrasion test on the semiconducting polymers with polytetrafluoroethylene (PTFE) as the stiff object causing the abrasion. (**B**) Schematic diagram showing the abrasion test on the semiconducting polymers with a porcine skin as the stiff object causing the abrasion. (**C**) Photographs showing a BASC film and a p(g2T-T) film before and after abrasion by a porcine skin under 1 kPa for 20 cycles. The arrows indicate the direction of the abrasion. (**D**) Changes of OECT on-current from the two films after the abrasion cycles perpendicular to the charge transport direction. Values represent the mean and the standard deviation (n = 5).

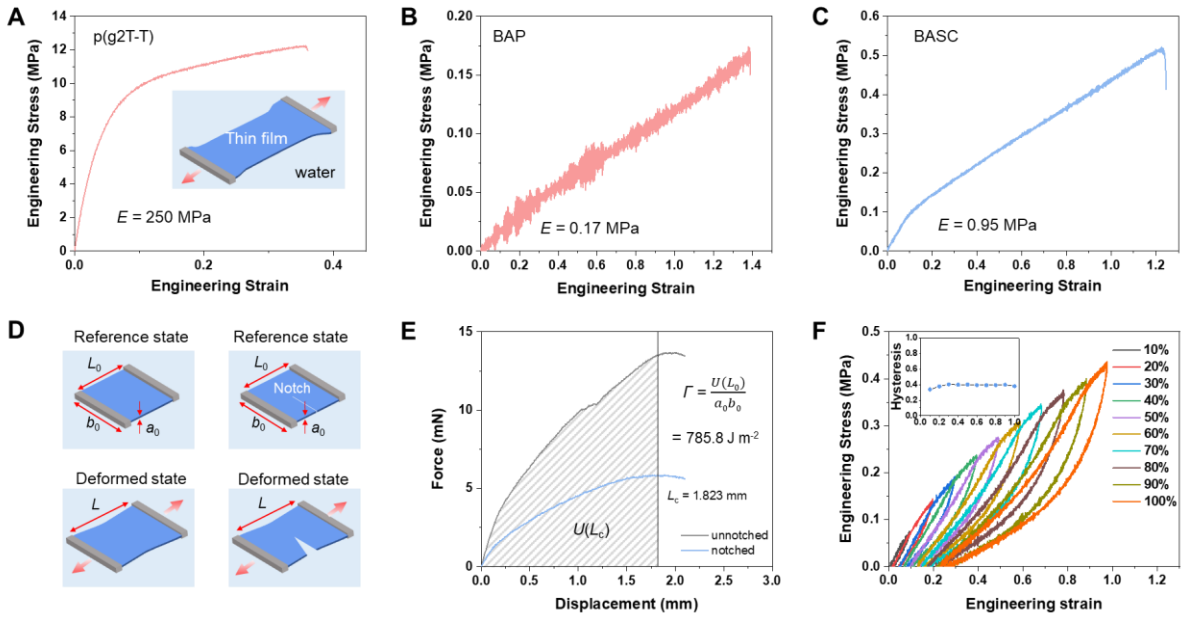

Fig. S26. Tensile strength, fracture toughness, and fatigue properties tested using a pseudo-freestanding tensile method (i.e., film-on-water (FOW) method). (**A**) Stress-strain curve of a neat p(g2T-T) film. (**B**) Stress-strain curve of a neat BAP film. (**C**) Stress-strain curve of a BASC film. (**D**) Schematic illustration of pure-shear test for an unnotched sample and a notched sample. (**E**) Force vs. displacement curve for fracture toughness measurement. L_c indicates the critical distance between the clamps at which the notch turns into a running crack. The measured fracture toughness of the bioadhesive semiconductor is 785.8 J m^{-2}. (**F**) Cyclic stretching tests at different strains. The inset shows the hysteresis for different strains.

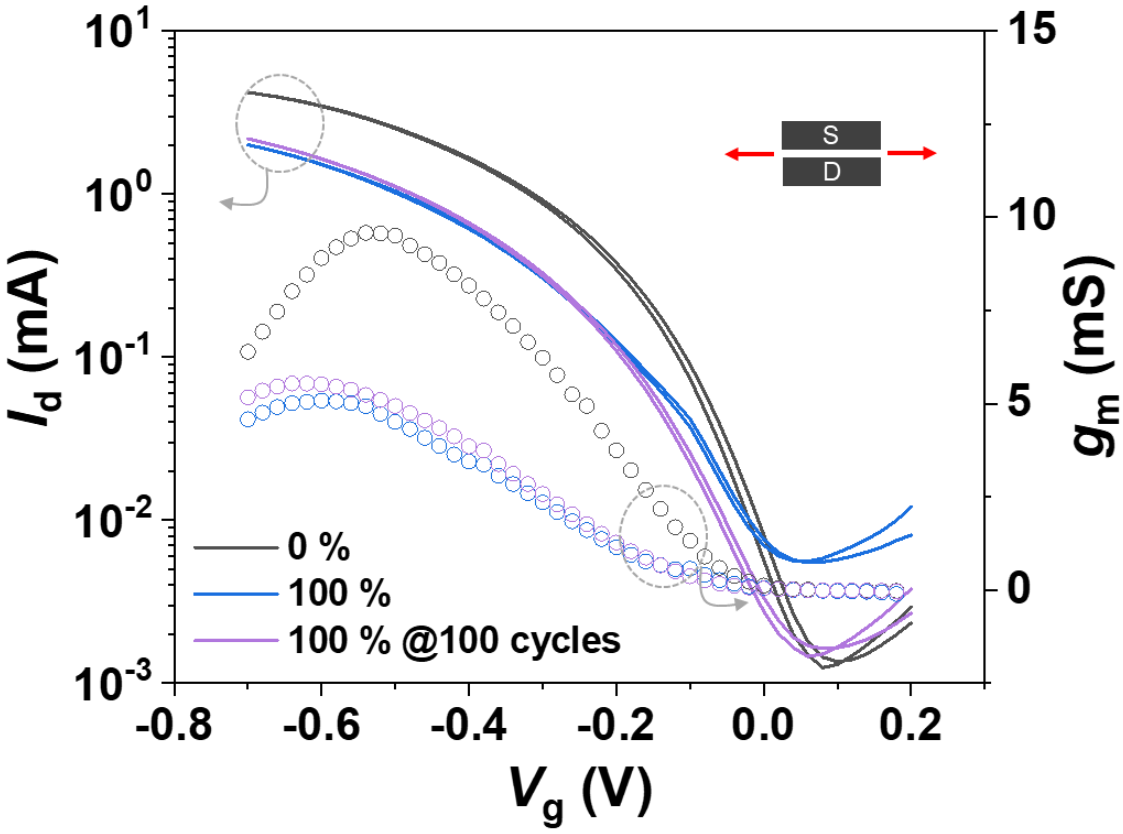

Fig. S27. OECT electrical performance of the BASC film stretched at 0 % strain, 100 % strain, and 100 % strain after 100 stretching cycles in the perpendicular direction. The measurement was done with V_d at -0.6 V.

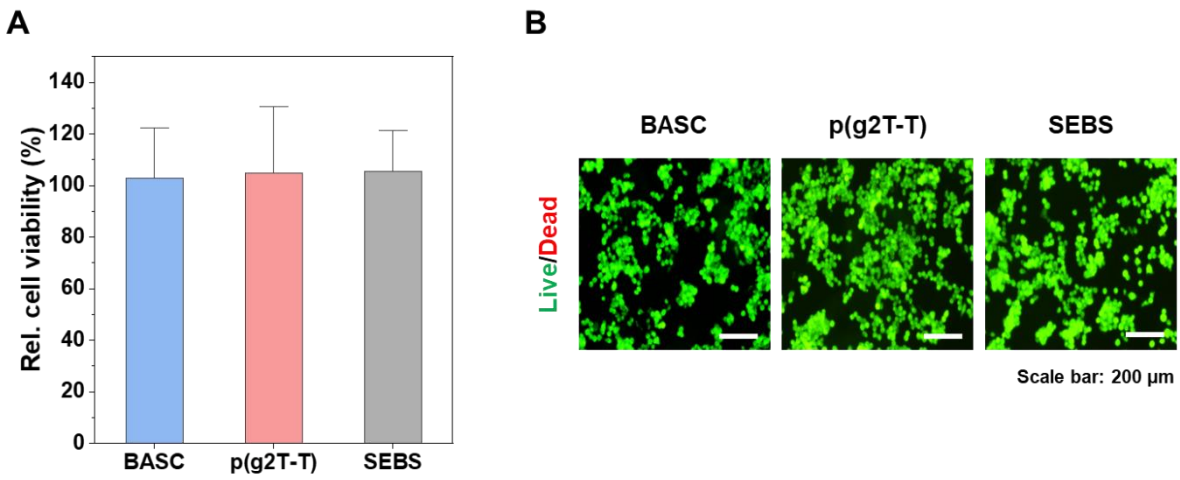

Fig. S28. Cell viability test of RAW cells after 24 h of culture. (**A**) MTT assay. (**B**) Live/Dead assay. The results show good biocompatibility of BASC films with comparable cell viability among the three groups and no signs of cell death.

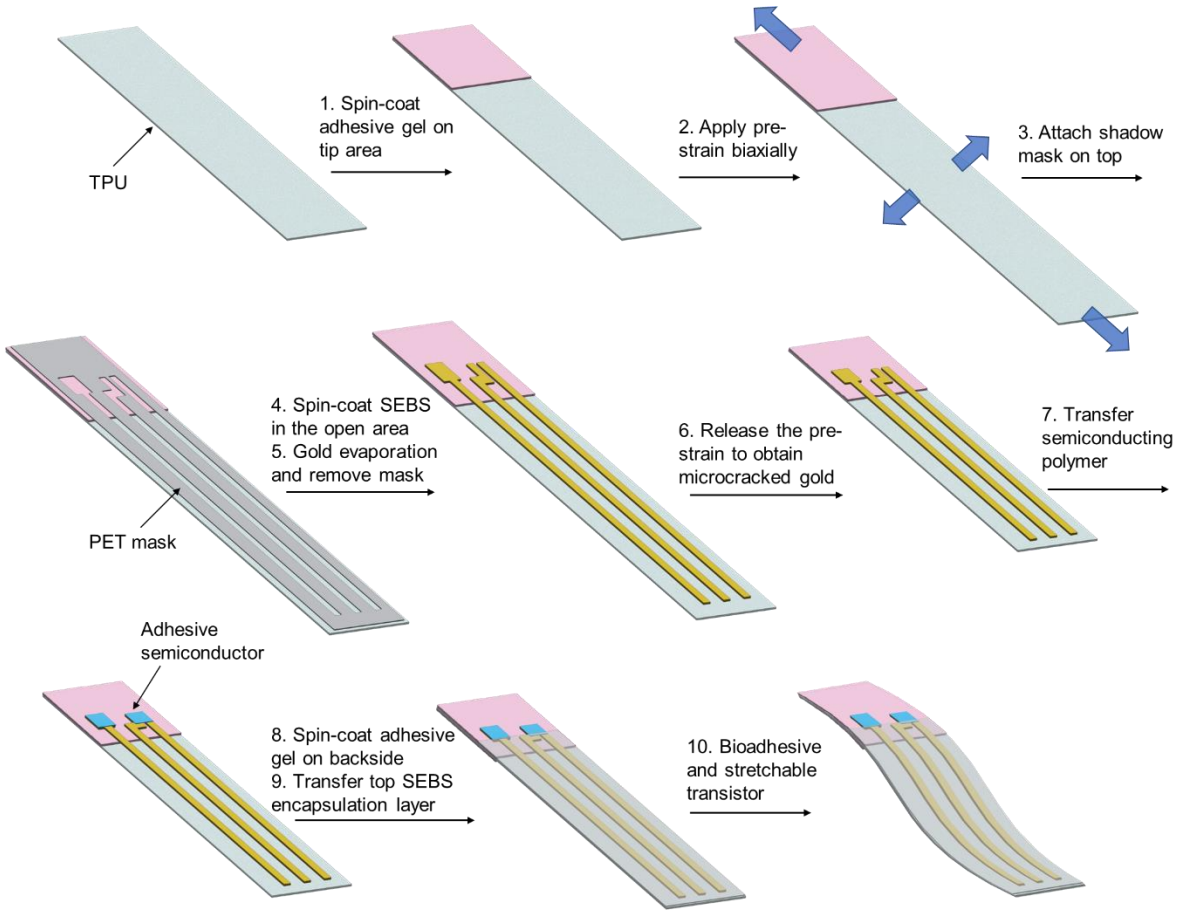

Fig. S29. Fabrication process of the fully bioadhesive OECT sensor.

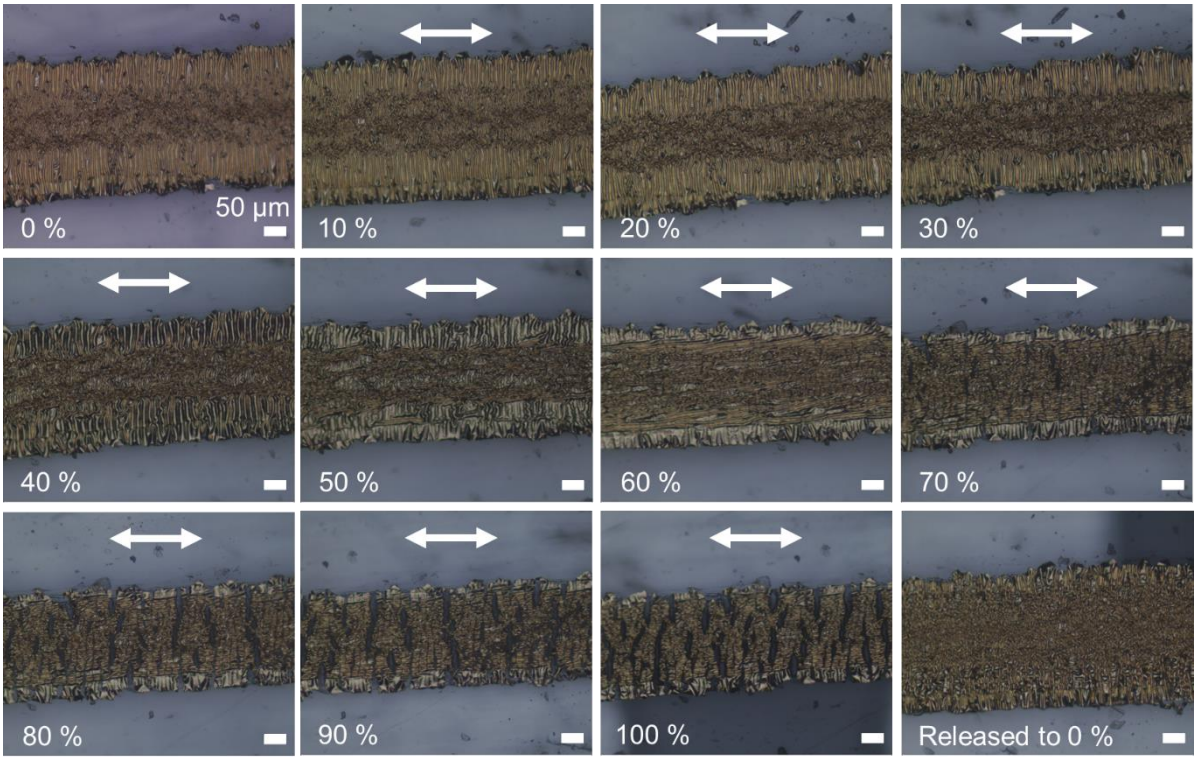

Fig. S30. Stretchability of the fabricated micro-crack gold electrodes. Optical microscopic images of the fabricated gold electrodes on BAP substrates at different strains. The substrate is pre-stretched at 80 % strain and the gold deposition rate is 1 Å/s. The gold thickness is 80 nm.

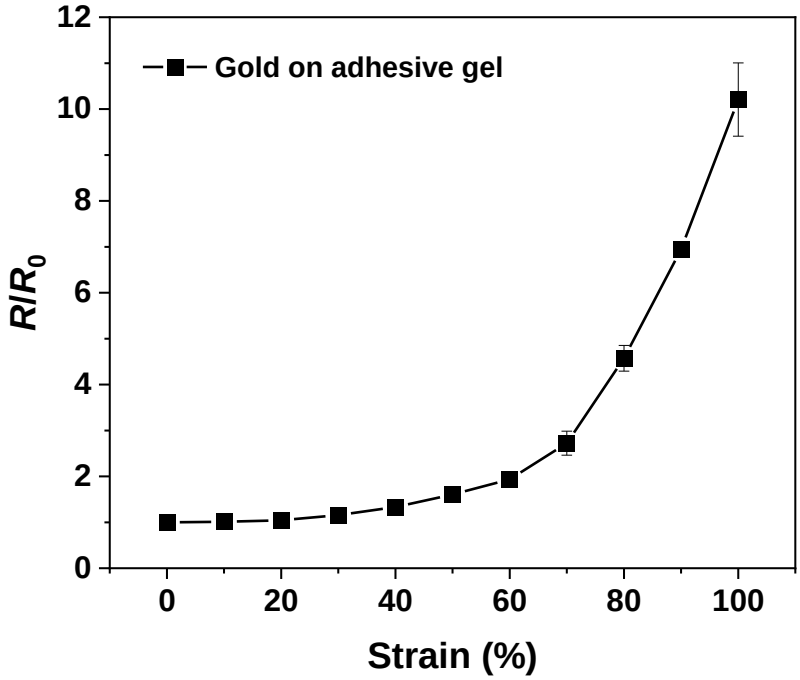

Fig. S31. Electrical resistance changes of micro-crack stretchable gold electrodes during stretching. The initial length, width and thickness of the gold electrode are 15 mm, 0.29 mm and 80 nm, respectively.

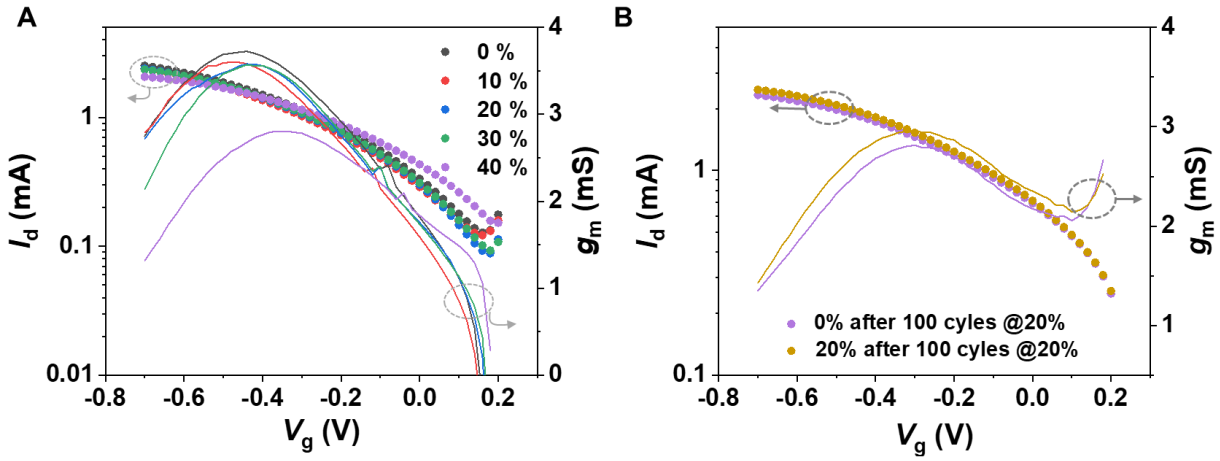

Fig. S32. Electrical performance of the fully bioadhesive OECTs during stretching. (**A**) Transfer curves for a fully-bioadhesive OECT from 0 % to 40 % strain. (**B**) Transfer curves for a fully-bioadhesive OECT during repeated stretching cycles.

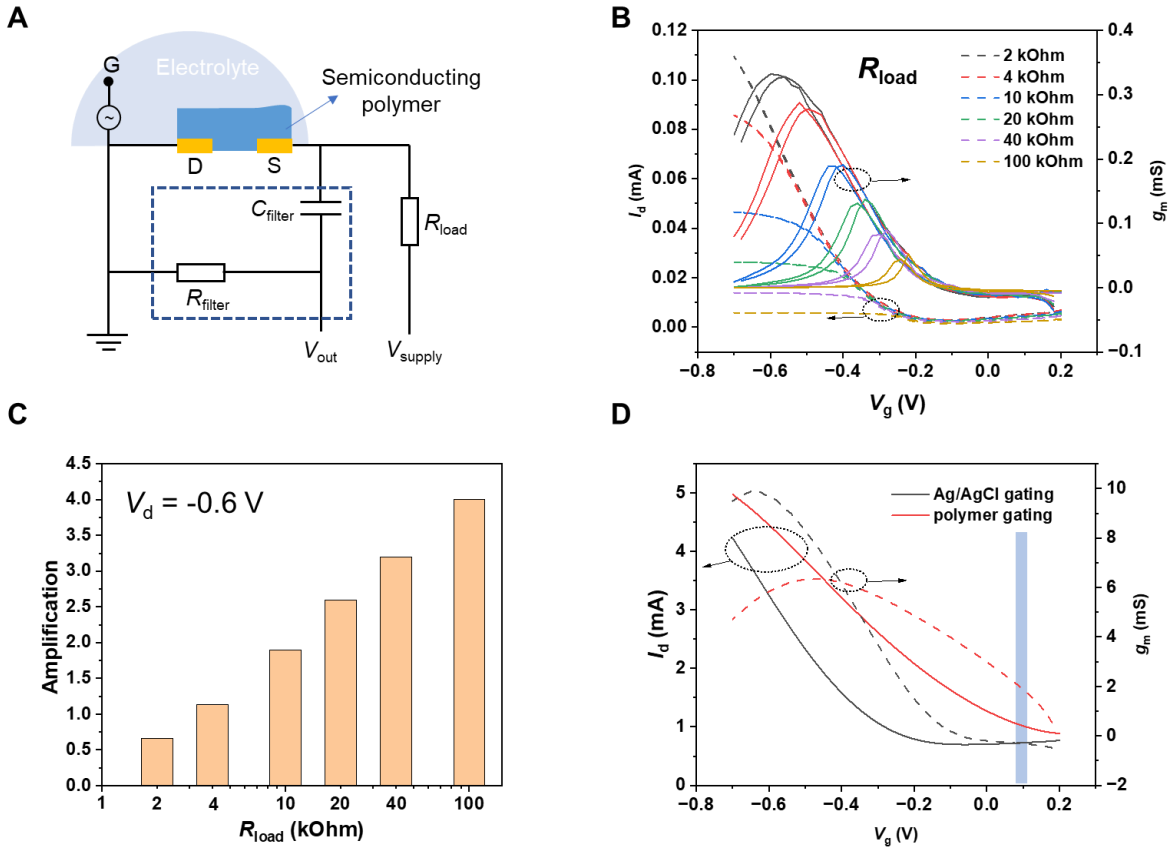

Fig. S33. OECT filtering and amplification circuit and performance. (A) Circuit diagram. The high-pass filter is composed of a capacitor C_{filter} (100 nF) and a resistor R_{filter} (1.5 MΩ). The high-pass frequency f_{filter} here is 0.15 Hz. The R_{load} is 22 kΩ. **(B)** OECT transfer curves with different load resistors R_{load}. **(C)** Calculated amplification (= $g_m \times R_{load}$) for the OECT with different R_{load}. **(D)** OECT transfer curves from two gating materials: the rigid Ag/AgCl electrode and the same semiconducting polymer. The polymer gating gives a higher transconductance g_m at V_g = 0 V.

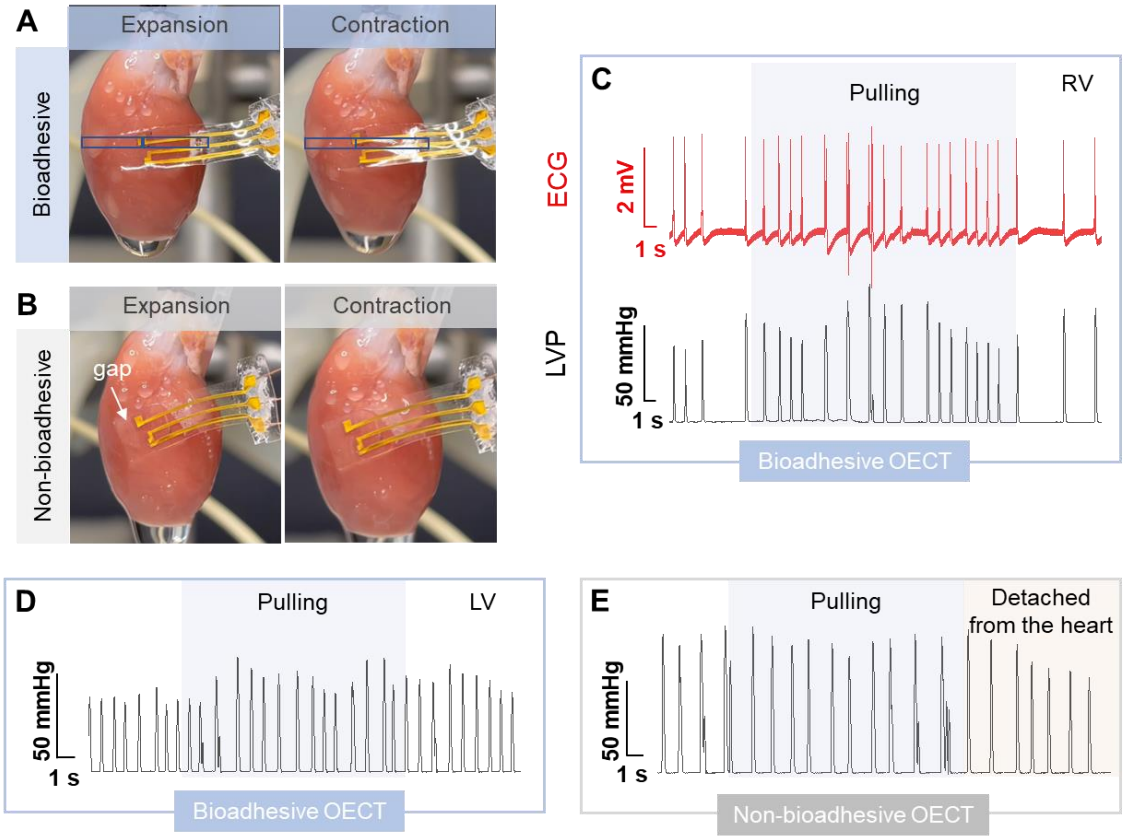

Fig. S34. ECG recording using OECT. (**A**) Photographs showing a fully-bioadhesive OECT attached to an isolated rat heart surface maintaining stable contact during heartbeats. (**B**) Comparison of a non-bioadhesive OECT, for which capillary-based attachment cannot maintain conformable and stable contact. (**C**) ECG signals recorded by the fully-bioadhesive OECT on the RV, accompanied with the ventricle pressures (bottom). (**D**-**E**) LVP recordings during the ECG measurement for the bioadhesive OECT (**D**) corresponding to Fig. 5G, and the non-bioadhesive OECT (**E**) corresponding to Fig. 5H.

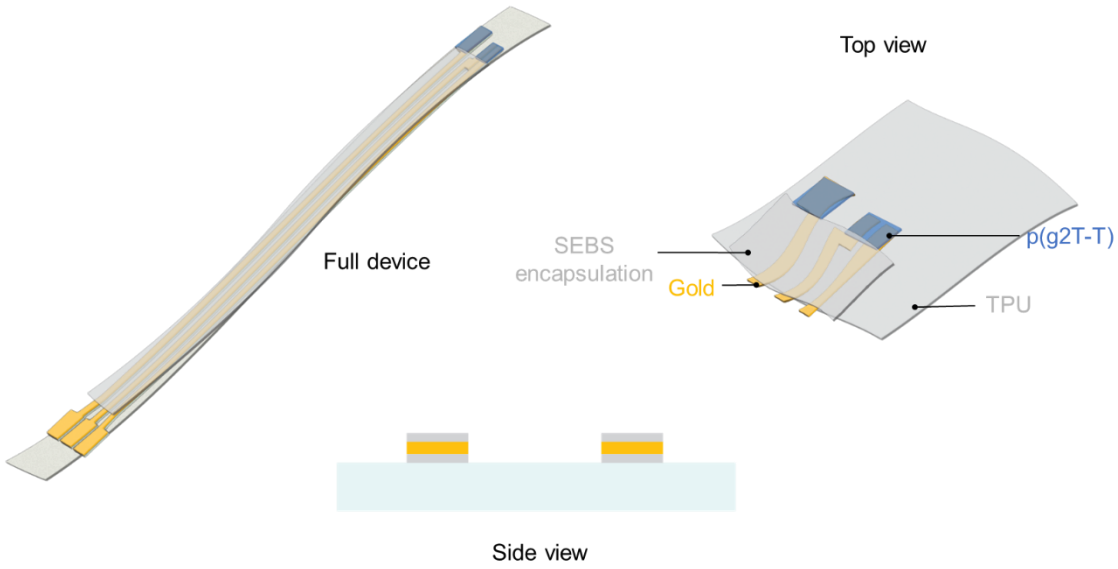

Fig. S35. Device structure of the non-bioadhesive OECT.

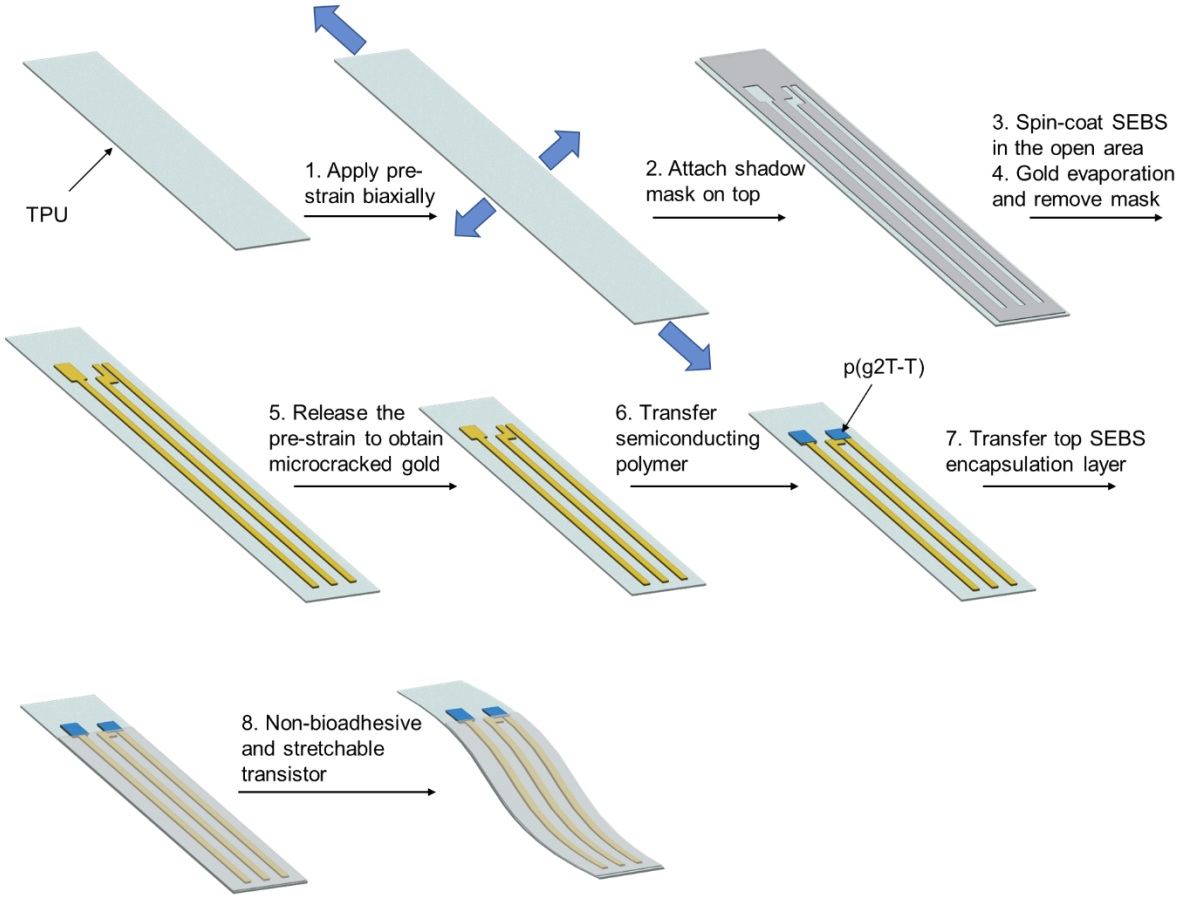

Fig. S36. Fabrication process of the non-bioadhesive OECT.

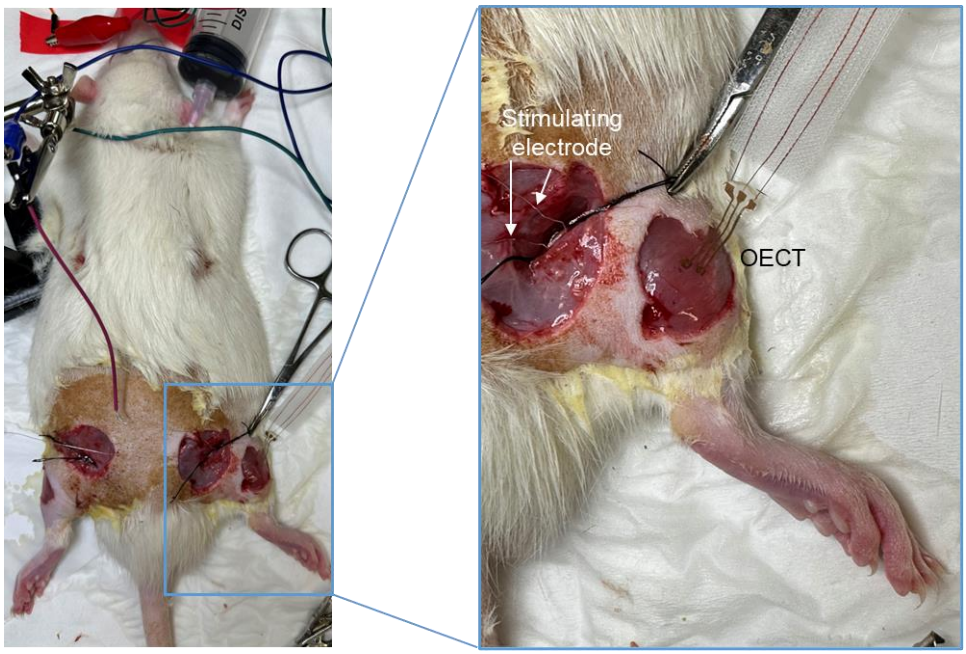

Fig. S37. Overview of the experimental setup for in vivo EMG recording. The sciatic nerve was stimulated by bipolar silver wire electrodes. The bioadhesive OECT was adhered to the gastrocnemius medialis (GM) muscle for EMG recording.

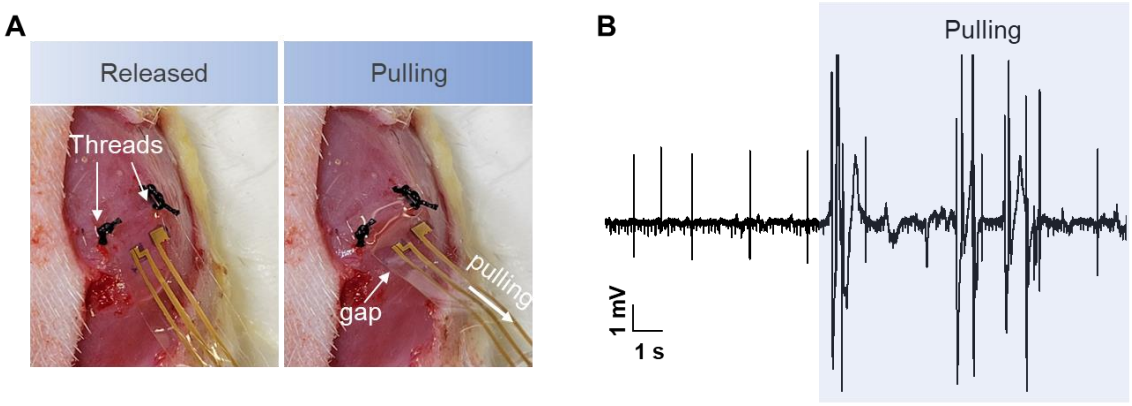

Fig. S38. Comparison of suturing-based fixation for an OECT device. (**A**) Suturing a non-bioadhesive OECT on the gastrocnemius medialis (GM) muscle causes tissue damages and bleeding, but cannot maintain conformable contact. (**B**) Recorded EMG signals showing inferior stability.

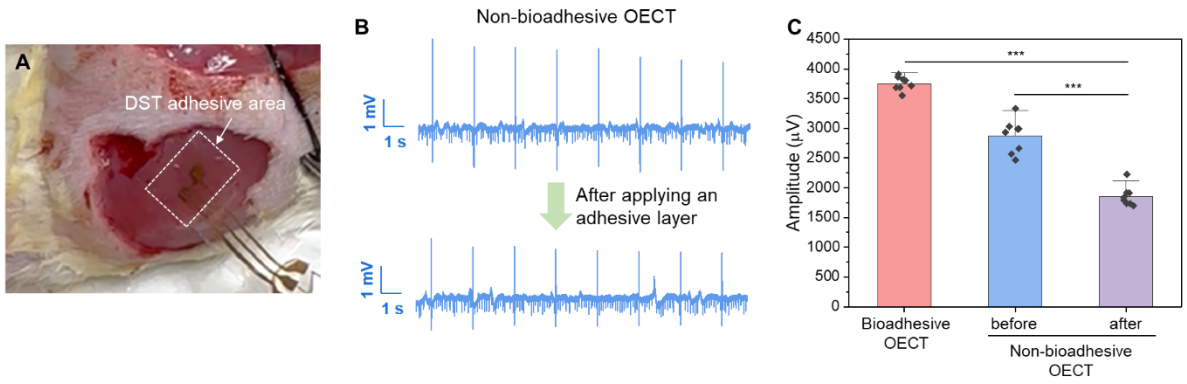

Fig. S39. Comparison of transistors for tissue interfacing with state-of-the-art adhesives. (**A**) The use of gelatin-based double-sided tape (DST) (*29*) as a separate adhesive layer between the non-bioadhesive transistor and the GM muscle for EMG recording. The dry thickness of the DST film is 140 μm. (**B**) The recorded EMG signals for the non-bioadhesive transistor before and after applying the DST adhesive layer between the GM muscle and the transistor. (**C**) Comparison of the signal amplitude recorded from the bioadhesive OECT, the non-bioadhesive OECT before and after applying the DST adhesive. Statistical significance and *P* values are determined by two-sided Student's t-test: ****P*<0.001.

Advantages of introducing bioadhesive properties to semiconductors and OECTs

In general, achieving direct adhesive between an OECT (in particular, its semiconducting channel) and tissue surface can give three folds of highly important advantages, as summarized below.

- Higher signal amplitudes and signal-to-noise ratios. As shown in Fig. S39, without the use of a tissue adhesive layer that increases the physical distance between a sensing device and tissue surface, the acquired signal amplitude can be doubled. This observation is consistent with a few other papers (*37-40, 52*) that studied the decays of biosignals transmitted in cells and tissues. It should be noted that according to the paper reporting the dry double-side adhesive (*29*), the thinnest dry tape thickness is 20 μm, which may reach 200 μm after swelling. Further reducing the hydrogel thickness might decrease the adhesion performance due to insufficient bulk dissipation mechanism (*53*, *54*). Therefore, the use of separate adhesive will inevitably lead to the increase of the device tissue distance by a certain amount.
- Improved spatial resolution. To understand cellular functions and network dynamics, one goal is to achieve single-cellular sensing resolution, which may reach several micrometers. Previous research (*55, 56*) has suggested electric potential rapidly decreases with increasing distance for small cellular current sources. This indicates single-cellular recording will become more challenging for an additional coating layer at the interface. Another influence on achieving high spatial resolution is the crosstalk among cells (*57, 58*). To achieve single cellular recording, not only should one shrink down the device size but also make close enough contact between the bioelectronic device and cells. Adding another adhesive layer will inevitably increase the sensing distance and thus the crosstalk among adjacent cells, which complicates the signal analysis.
- Ease of device attachment and surgical processes. First, the incorporation of tissue-adhesive properties to the semiconducting layer avoids the preparation of a separate adhesive tape or coating. which requires that the dry adhesive is in a certain dimension and is also adhesive to the devices. Second, it avoids the additional consideration and evaluation about the cytotoxicity and inflammatory response from the separate adhesive layer. Third, the device attachment process to tissue surface now becomes just one step of directly pressing the device to the tissue surface, rather than a two-step process including first attaching a tissue adhesive, and then attaching a device. With the swelling process of the tissue adhesive happening instantaneously, such a two-step process becomes even more complicated and could lead to compromised device attachment. In comparison, the one-step attachment of an intrinsically bioadhesive device can maximize the success rate of attaching to the desired location and achieve the most conformable interface.

In summary, direct and intimate biointerfaces using bioadhesive semiconductors and transistors provide the advantages of higher sensing amplitude, improved sensing spatial resolution, and ease of operation.

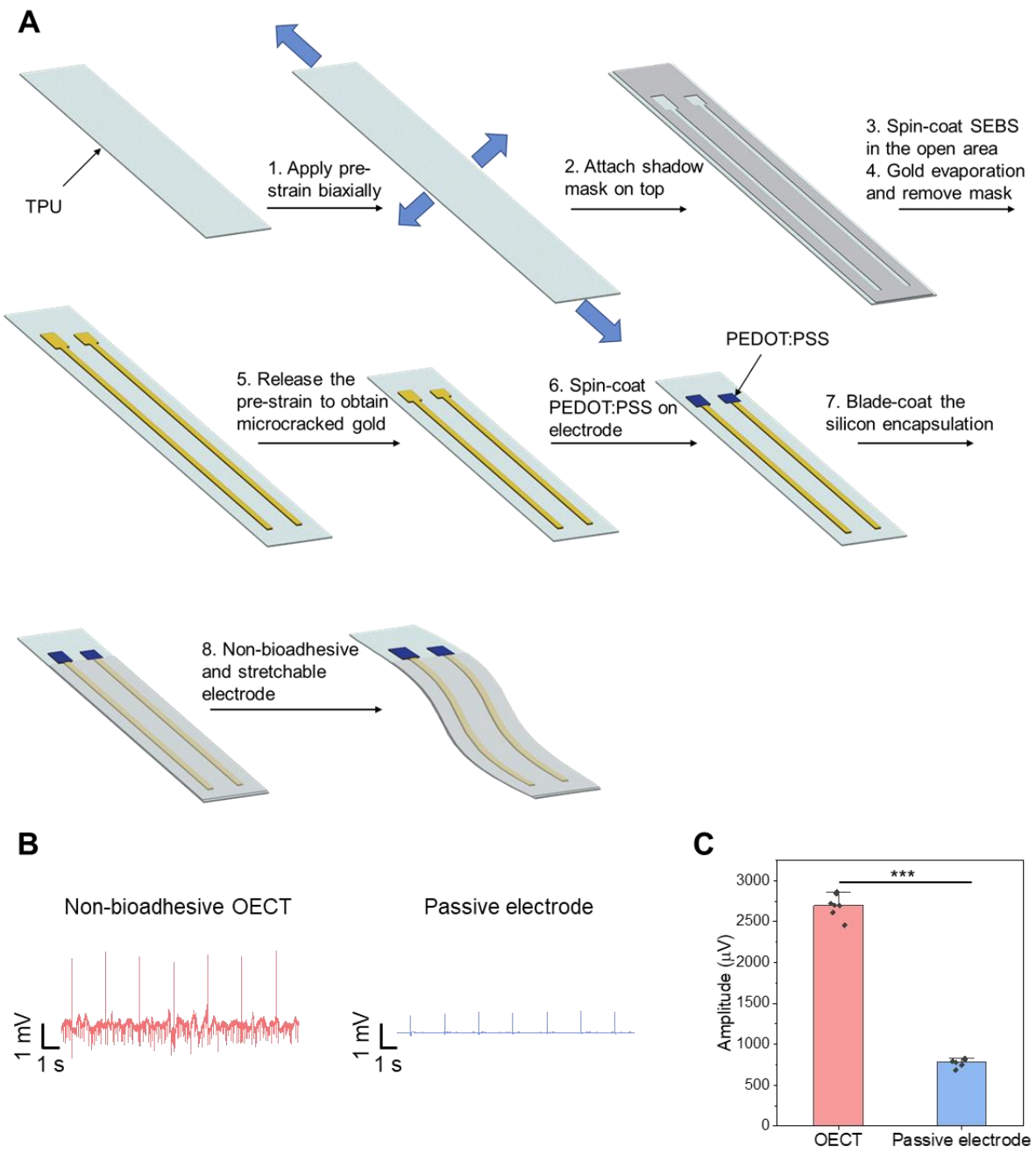

Fig. S40. Signal amplitude comparison of the bioadhesive transistor with the passive electrode based on PEDOT:PSS. (**A**) Fabrication process of the passive electrode based on PEDOT:PSS coating. (**B**) EMG recording from the non-bioadhesive OECT and the passive electrode on the GM muscle. (**C**) Comparison of the signal amplitude recorded from the non-bioadhesive transistor and passive electrode. Statistical significance and *P* values are determined by two-sided Student's t-test: ****P*<0.001.

Table S1. Molecular weights of the utilized conjugated polymer

Polymers	M_n (kDa)	M_w (kDa)	PDI
p(g2T-T)	36	63	1.7

Table S2. Summary of adhesive polymer compositions

	p(g2T-T)	ACTEGCOOH	ACTEGNHS
BASC	1	20	20
BASC-COOH	1	40	0
BASC-NHS	1	0	40
BAP	0	20	20
BAP-COOH	0	40	0
BAP-NHS	0	0	40

*The values show the weight ratios.

Table S3. Comparison of the adhesion performances of bioadhesive electronic materials

	Composition	Format	Interfacial toughness[a] (J/m^2)	Shear strength[a] (kPa)	Tensile strength[a] (kPa)	Adhesion time[b]	Ref.
Bioadhesive conductor	PEDOT:PSS P(AAc-*co*-NHS)	Double layer structure	230	N/A	N/A	5 s/24 h	(*60*)
	PEDOT + polydopamine	blending	N/A	~3.5	N/A	N/A	(*14*)
	rGO + p(AAc-*co*-NHS)	blending	230	50	N/A	5 s/24 h	(*16*)
	Graphite + poly(SBVI)	blending	N/A	52 (porcine skin)	N/A	10 min	(*15*)
	PEDOT:PSS + pSB	blending	98.7	N/A	N/A	30 s	(*61*)
Neat semiconductor	P(g2T-T)	neat	2.9	1.2	2	1 min/2 h	This work
Bioadhesive semiconductor	P(g2T-T) + BAP	blending	24	6.8	4.4	1 min/2 h	This work

[a] Unless noted, the adhesion performance was measured on porcine muscles.
[b] The adhesion time was reported as pressing time/storage time before mechanical measurements. Otherwise, only pressing time is given.
P(AAc-*co*-NHS)-P(acrylic acid-*co*- *N*-hydroxysuccinimide ester); rGO-reduced graphene oxide; poly(SBVI)-poly(sulfobetaine vinylimidazolium); pSB-poly(sulfobetaine).
N/A-Not available.

Table S4. Comparison of the OECT performances of polymer semiconductors

Materials	Type	μ[a] ($cm^2\ V^{-1}\ s^{-1}$)	C^* ($F\ cm^{-3}$)	μC^*[a] ($F\ cm^{-1}\ V^{-1}\ s^{-1}$)	V_{th} (V)	On/off ratio	Ref.
P3MEEMT	P	0.28	175	49	-0.6	N/A	(*62*)
P(g2T-TT)	P	1.08	241	261	-0.2	~10^5	(*33*, *63*)
P(g2T2-g4T2)	P	2.79	187	522	0.02	~10^5	(*64*)
PEDOT:PSS	P	1.2	39	47	0.4	~10^5	(*33*, *65*)
Crys-P	P	4.34	113	490	N/A	N/A	(*66*)
P(bgDPP-MeOT2)	P	1.6	120	195	-0.33	~10^5	(*67*)
P(gDPP-T2)	P	1.74	196	342	-0.5	~10^5	(*68*)
BBL	N	0.0007	930	0.65	0.35	~10^4	(*69*)
P(gNDI-gT2)	N	0.00045	397	0.18	0.35	~10^3	(*70*)
PgNaN	N	0.00662	100	0.662	0.37	~10^4	(*71*)
NDI-T2 (P-90)	N	0.000238	198	0.047	0.25	~10^3	(*72*)
P(g2T-T)	P	0.76	220	167	-0.2	~10^5	(*32*)
Bioadhesive semiconductor	P	1.01	2.9	2.9	0.07	~10^4	This work

[a]μ and μC^* are calculated data from the equation $g_m = \frac{Wd}{L}\mu C^*(V_{th} - V_g)$,
where $\frac{Wd}{L}$ is the device geometrical parameter.
N/A- Not available

Movie S1. ECG measurement on a rat heart using a bioadhesive OECT. The bioadhesive OECT was adhered to the ex vivo rat heart and could maintain stable contact during heartbeats and mechanical agitation.

Movie S2. ECG measurement on a rat heart using a non-bioadhesive OECT. The non-bioadhesive OECT was attached to the ex vivo rat heart. Air gaps existed between the OECT and the heart surface. The non-bioadhesive OECT slid on and was detached from the heart surface when the pulling force was applied.

Movie S3. EMG measurement on the GM muscle using a bioadhesive OECT. The bioadhesive OECT was adhered to the in vivo rat GM muscle and showed stable interfacing when the pulling force was applied and during the electrical stimulation of the sciatic nerve.

Movie S4. EMG measurement on the GM muscle using a non-bioadhesive OECT. The non-bioadhesive OECT was attached to the in vivo rat GM muscle. The non-bioadhesive OECT slid on and finally was detached from the muscle when pulling force was applied.